

International Journal of Fatigue

Experimental analysis of the plastic CTOD to characterize the variable amplitude fatigue crack growth in Grade 2 titanium samples

--Manuscript Draft--

Manuscript Number:	IJFATIGUE-D-23-00253R2
Article Type:	Original Research Paper
Keywords:	Fatigue crack growth; grade 2 titanium; Overload; DIC; CTOD
Corresponding Author:	Giancarlo L. Gómez Gonzáles, D.Sc. University of Jaen Jaén, Andalucía SPAIN
First Author:	Giancarlo L. Gómez Gonzáles, D.Sc.
Order of Authors:	Giancarlo L. Gómez Gonzáles, D.Sc. Jose M. Vasco Olmo Fernando V. Antunes Diogo M. Neto Francisco A. Díaz
Manuscript Region of Origin:	Europe
Abstract:	In this paper, the plastic component of the crack-tip opening displacement (CTOD _p) is experimentally evaluated to characterize the fatigue crack growth behavior in a Grade 2 titanium sample under single overload with constant amplitude loading conditions. The CTOD measurements were performed with the 2D-Digital Image Correlation (DIC) technique. The experimental results show a linear correlation between CTOD _p and fatigue crack growth rates, suggesting the independence of this relationship to load-interaction effects. Therefore, this study demonstrates that the CTOD _p can be a suitable crack-driving parameter to study crack propagation behavior under variable amplitude loading. Furthermore, it suggests that the fatigue crack growth process is primarily caused by cyclic plastic deformation.
Suggested Reviewers:	Tomáš Vojtek Institute of Physics of Materials Czech Academy of Sciences vojtek@ipm.cz Recent publication studying CTOD Jaroslav Pokluda Brno University of Technology pokluda@fme.vutbr.cz He studies mechanisms of Fracture and Fatigue Thomas Seifert Offenburg University thomas.seifert@hs-offenburg.de
Response to Reviewers:	Thank you for giving us the opportunity to submit a revised draft of our manuscript for publication in the International Journal of Fatigue. We appreciate the time and effort that you and the reviewers dedicated to providing feedback on our manuscript and are grateful for the insightful comments on and valuable improvements to our paper. We have incorporated the suggestions made by the reviewers. Those changes are highlighted within the revised version of the manuscript.

G.L. Gómez Gonzales*, J.M. Vasco-Olmo, F.V. Antunes, D.M. Neto, F.A. Díaz. Experimental analysis of the plastic CTOD to characterize the variable amplitude fatigue crack growth in Grade 2 titanium samples. International Journal of Fatigue, 174: 107728, 2023. T1, Q1 (15/183 en Mechanical Engineering, IF 2023: 5.7). <https://doi.org/10.1016/j.ijfatigue.2020.105567>.

Highlights:

Experimental analysis of the plastic CTOD using the DIC technique.

Study of the plastic CTOD behavior under single overload with constant amplitude loading conditions.

Observations of the plastic behavior in the crack tip region.

Experimental data for understanding the mechanisms governing the fatigue crack growth process.

Experimental analysis of the plastic CTOD to characterize the variable amplitude fatigue crack growth in Grade 2 titanium samples

Giancarlo L. Gómez Gonzales^a, Jose M. Vasco-Olmo^a, Fernando V. Antunes^b, Diogo M. Neto^b,
Francisco A. Díaz^a

^aDepartamento de Ingeniería Mecánica y Minera, University of Jaén, Jaén, Spain.

^bDepartment of Mechanical Engineering, Centre for Mechanical Engineering, Materials and Processes (CEMMPRE), University of Coimbra, Coimbra, Portugal.

Abstract

In this paper, the plastic component of the crack-tip opening displacement (CTOD_p) is experimentally evaluated to characterize the fatigue crack growth behavior in a Grade 2 titanium sample under single overload with constant amplitude loading conditions. The CTOD measurements were performed with the 2D-Digital Image Correlation (DIC) technique. The experimental results show a linear correlation between CTOD_p and fatigue crack growth rates, suggesting the independence of this relationship to load-interaction effects. Therefore, this study demonstrates that the CTOD_p can be a suitable crack-driving parameter to study crack propagation behavior under variable amplitude loading. Furthermore, it suggests that the fatigue crack growth process is primarily caused by cyclic plastic deformation.

Keywords: Fatigue crack growth, grade 2 titanium, overload, DIC, CTOD

Nomenclature

2D	bidimensional dimension
CT	compact tension
CTOD	crack tip opening displacement
CTOD _p	plastic CTOD
E	Young's modulus
F	applied force
FCG	fatigue crack growth
K	stress intensity factor
OL	overload
PICC	plastic-induced crack closure
R	load ratio
U*	crack closure level
v	vertical displacement
α	numeric constant
Δ CTOD _p	range of plastic CTOD
Δ K	stress intensity factor range

ΔK_{eff}	effective stress intensity factor range
$\Delta \varepsilon$	strain range
$\Delta \sigma$	stress range
ε	strain
$\varepsilon_y, \varepsilon_{cy}$	yield strain, cyclic yield strain
σ	stress
σ_y, σ_{cy}	yield stress, cyclic yield stress

1. Introduction

Despite the numerous studies [1-8] devoted to understanding the phenomenon of fatigue crack growth (FCG) under different loading conditions, the prediction of fatigue life in real engineering structures with crack-like defects remains challenging. This results from the difficulty of developing a universal equation to describe the load sequence effects taking into account all the complex mechanisms involved in the FCG process. This concerns, for example, plasticity-induced crack closure (PICC), crack roughness, crack closure induced by corrosion, residual stresses, crack blunting and crack branching, among others.

Although the small-scale cyclic plasticity at the crack tip due to cyclic loading can be successfully described with the stress intensity factor range, ΔK , the FCG rates (da/dN) vs ΔK relation proposed by Paris and Erdogan [9] does not account for mean stress effects (described by the R-ratio) and load-interaction or load-history effects. In fact, Paris's law is often used to assess experimental FCG rates vs ΔK data from constant amplitude loading fatigue tests whereas real engineering components are commonly submitted to non-uniform loading. Instead of using the ΔK , Elber [2] proposed the effective stress intensity factor range, ΔK_{eff} , which is affected by crack closure under a certain load level, i.e. $\Delta K_{\text{eff}} = K_{\text{max}} - K_{\text{open}}$ where K_{max} is the maximum stress intensity and K_{op} is the stress intensity at the crack opening. The crack closure concept became popular in literature since it can justify the effects of stress ratio and load history on fatigue crack propagation. However, it is still a topic of research and discussion within the fatigue community [10-14], as studies continue to be conducted to investigate the actual role of the crack closure mechanism in fatigue crack propagation.

In this context, non-linear parameters such as the CTOD_p, dissipated energy, J-integral, and plastic strain range have been suggested to correlate the crack-tip damage since they can effectively quantify the crack-tip plasticity. According to Antunes et al. [15], there are well-defined relationships between these parameters, as they all quantify the same phenomenon: the crack tip plastic deformation which is believed to be the main mechanism of fatigue crack growth. Nowadays, improved experimental techniques and numerical methods have made it possible to examine the near-tip region more closely, where the non-linear fatigue damage effectively occurs. Pokluda et al. [16] and Chen et al. [17] proposed the use of the

1
2
3
4
5
6
7
8
9
10
11
12
13
14
15
16
17
18
19
20
21
22
23
24
25
26
27
28
29
30
31
32
33
34
35
36
37
38
39
40
41
42
43
44
45
46
47
48
49
50
51
52
53
54
55
56
57
58
59
60
61
62
63
64
65

cyclic plastic strain range. Heung et al. [18] linked FCG with the cyclic plastic zone size, while Zhang et al. [19] conducted a numerical analysis, concluding that FCG can be correlated with the size of the monotonic plastic zone. Bodner et al. [20] and Klingbeil et al. [21] used the total dissipated energy as the crack driving force parameter to describe fatigue crack growth in ductile solids. In particular, the CTOD is an important fracture mechanics parameter used to characterize the local crack opening and closing, proving a physical meaning to the progressive crack extension under cyclic loading that occurs in yielding materials. The proportional relationship of the cyclic CTOD with the crack propagation rate (i.e. da/dN) has been proposed and experimentally and numerically investigated in a large number of papers, e.g. [22-29].

The significance of the plastic component of the CTOD ($CTOD_p$) was studied by Antunes et al. [30] through numerical experiments, showing its linear relationship with FCG rates in linear scales. They concluded that using the da/dN - $CTOD_p$ relation, the crack closure phenomenon, crack tip blunting, residual stresses, and fatigue threshold are included naturally. Furthermore, the independence of the da/dN - $CTOD_p$ relationship to the stress ratio for FCG tests was also verified by Antunes et al. [31] and Vasco et al. [32, 33] using FCG tests performed on aluminum and titanium specimens. In these studies, the CTOD measurements were obtained by DIC analysis, showing that only the plastic component on CTOD ($CTOD_p$) exhibits a consistent increase with FCG rates. These findings are equivalent to studies mentioned before in which the CTOD is measured directly at the crack tip, i.e. at a distance about CTOD behind the real blunted crack or at the position of the crack tip on the fracture surface of the last fatigue load cycle.

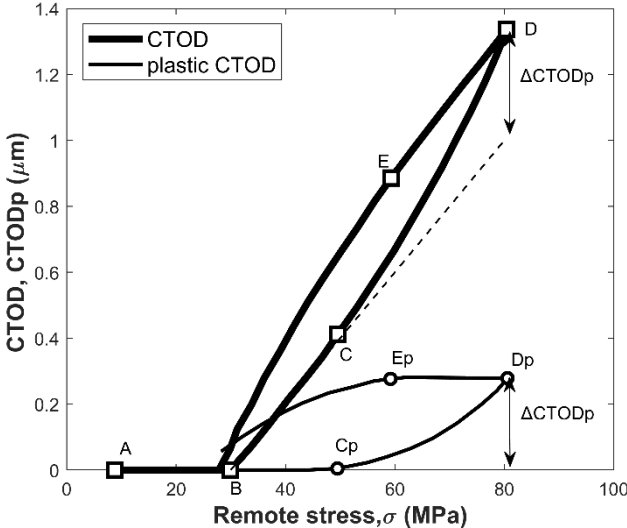
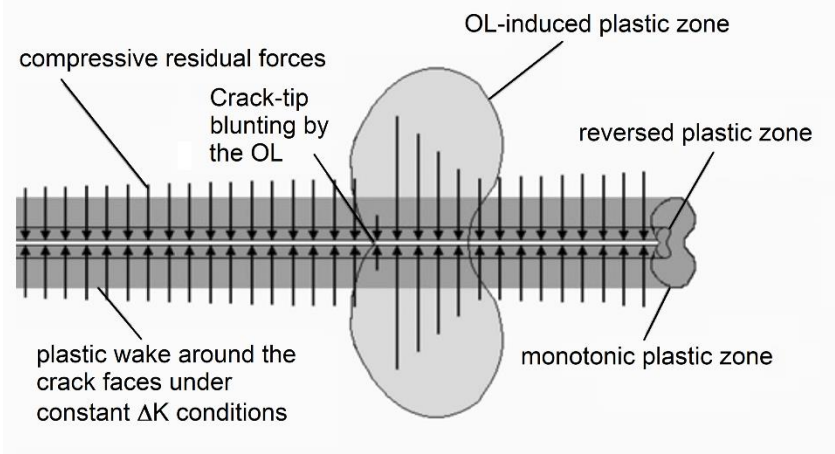


Figure 1. Variation of CTOD values throughout a full load cycle and determination of $CTOD_p$ [27].

1 Figure 1 shows the typical results obtained of total CTOD versus applied load from finite element
 2 simulation. Segment AB corresponds to the closed position of the crack. The crack opening and
 3 subsequent elastic behavior are observed in segment BC. As the loading is applied, plastic deformation is
 4 initiated during the segment CD. The value of the plastic CTOD ($CTOD_p$) is obtained after removing the
 5 elastic component from the total CTOD. For that, the extrapolation of the segment BC that corresponds
 6 to the elastic behavior of the material is required which is also parallel to the segment DE related to the
 7 elastic unloading. The evolution of plastic CTOD is also represented in Figure 1. $CTOD_p$ increases non-
 8 linearly from point C_p , which defines the end of the elastic regime, up to the maximum value registered
 9 at the maximum load (point D_p) defined by $\Delta CTOD_p$.

10 This paper follows the previous studies presented in Refs [31-33], exploring the applicability of the
 11 $CTOD_p$ parameter for the analysis of fatigue crack propagation after the application of a single overload
 12 (OL) during constant amplitude load. It is well known that one approach used to investigate the behavior
 13 of the mechanisms governing the FCG process consists in analyzing the effects caused by the imposition
 14 of simple load sequences such as single-cycle overload. The loading sequences can produce several load
 15 interaction effects, leading to acceleration or deceleration in fatigue crack growth rate. The significance
 16 of the non-linear parameters is that they can naturally accommodate the effects of load sequences, as well
 17 as stress state and specimen geometry, among others.



18 Figure 2. Scheme of Elber's OL-induced retardation.

19 It is well known that the imposition of a single peak overload retards the subsequent crack propagation
 20 for some period. Residual stresses ahead of the crack [7] and plasticity-induced crack closure acting on
 21 the crack surfaces [8] are identified as the main mechanisms for the crack retardation observed following
 22 overload application. As shown in the schematic of Figure 2, within the OL-induced plastic zone, larger
 23 residual stresses are generated which decrease from their maximum value to their initial value before the
 24 OL application. According to the PICC model, the effects caused by the OL event must cease after the

current plastic zone has left the region hypertrophied by the OL. However, studies [34,35] in the literature report OL-induced delay effects far away from the extension of the overload plastic zone, a phenomenon called discontinuous crack closure. Furthermore, crack propagation mechanisms may act concurrently or in competition, depending on a variety of factors like the crack extension, the material's microstructure, and the stress state, among others.

This investigation aims to study the fatigue crack behavior of Grade 2 titanium samples under overload conditions, and the feasible use of the $CTOD_p$ as a parameter for fatigue crack growth characterization. The CTOD measurements from the vertical displacement of the crack flanks, according to Mode-I (opening mode) were extracted using the 2D Digital Image Correlation (DIC) technique. Previous works [36, 37] reported its successful application to obtain CTOD measurements from multiscale experiments.

2. Experimental details

The FCG tests were conducted on a servo-hydraulic MTS testing machine (MTS machine with a load cell of 25 kN). The test samples were compact tension (CT) specimens machined from a 1mm thick sheet of Grade 2 titanium ($E = 105$ GPa and $\sigma_y = 390$ MPa). The specimen dimensions are provided in Figure 3a. The specimens were cycled at a cyclic frequency of 2 Hz under constant amplitude loading with a maximum level of 750 N and a stress ratio (R) of 0.1. Two samples were tested using the same loading conditions. In one of them, a single 50% tensile overload (i.e. a single cycle with a maximum loading of 1125 N) was applied manually after the crack reached a length of 6 mm (measured from the point of load application), and then constant amplitude loading was resumed (see Figure 3b).

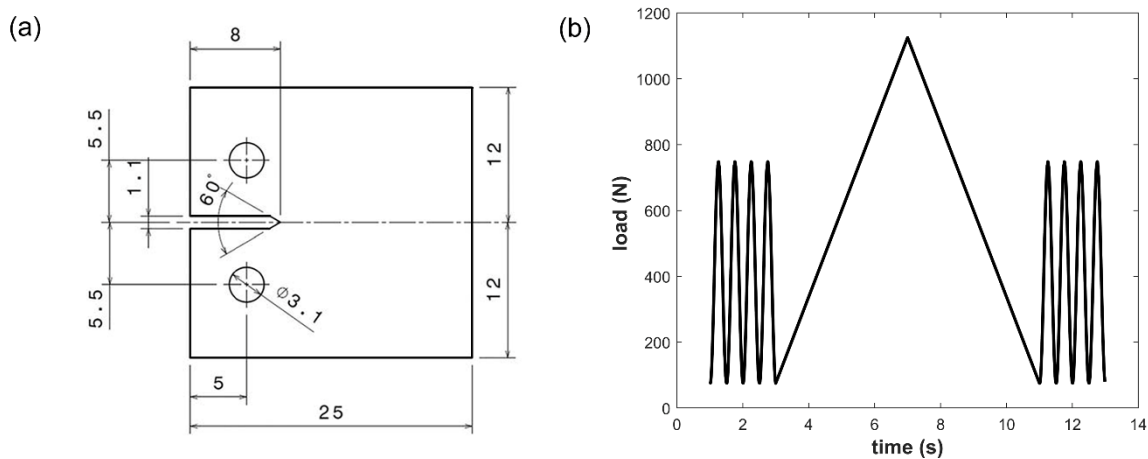
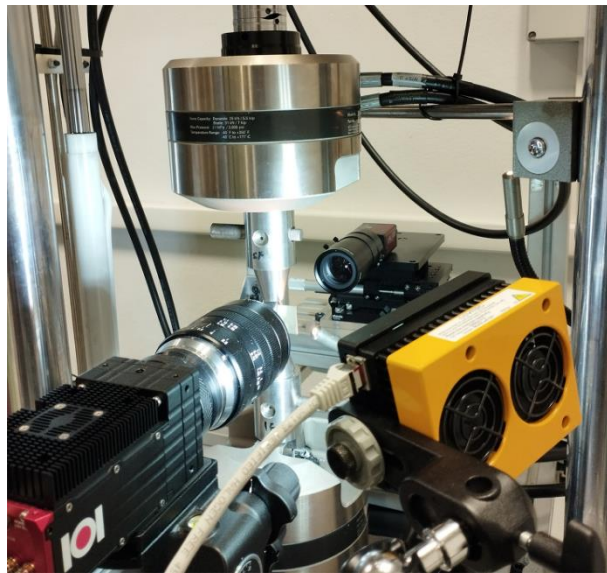


Figure 3. (a) Geometry of the sample (dimensions in mm), and (b) 2D-DIC setup used for investigation.

As mentioned earlier, the 2D-DIC analysis was adopted for investigation. For that, a high-resolution camera (Redwood 65MP sensor) coupled to high-magnification lenses (Laowa 60mm F2.8 2X) was located perpendicular to one face of the specimen. Besides, an additional camera (Stingray F-504B 5MP

1 sensor) was located in front of the other face to monitor the crack advance during the fatigue test, as shown
2 in the experimental setup of Figure 4. During the FCG test, the cameras were configured to take about
3 100 images from each loading cycle analyzed. All images captured from FCG tests were processed with
4 the commercial VIC-2D software from Correlated Solutions. The optical configuration achieves a spatial
5 resolution of 2 $\mu\text{m}/\text{pixel}$. The displacement resolution estimated from an uncertainty assessment, also
6 known as the noise floor [38], was 24 nm.
7
8
9



10
11
12
13
14
15
16
17
18
19
20
21
22
23
24
25
26
27
28
29
30
31
32
33
34
35
36
37
38
39
40
41
42
43
44
45
46
47
48
49
50
51
52
53
54
55
56
57
58
59
60
61
62
63
64
65
Figure 4. 2D-DIC setup used for investigation

2.1. Measurement of the plastic CTOD

Images of loading cycles captured at different crack lengths were processed by the DIC analysis software. In this analysis, the image registered at the minimum loading of each cycle was selected as the reference image. The DIC displacement maps, parallel to the load direction, were used to obtain the CTOD measurements according to Mode-I (opening mode).

The vertical displacement map provided by the DIC analysis at maximum loading for a crack length of 6 mm is depicted in Figure 5a. In this figure, the relative displacements are in agreement with the mode I of crack propagation or opening mode, in which the crack opens due to the application of stresses perpendicular to the plane in which it propagates. After the accurate localization of the crack tip, measurements of the crack opening–closing behavior are obtained by placing symmetrical points behind the crack tip at 0.1 mm from the flanks of the crack, as shown in Figure 5b. The relative displacement between the upper and lower crack flank is evaluated according to the following formula: $\text{CTOD} = v_{\text{upper}} - v_{\text{lower}}$, where v is the local measurement of the vertical displacement map.

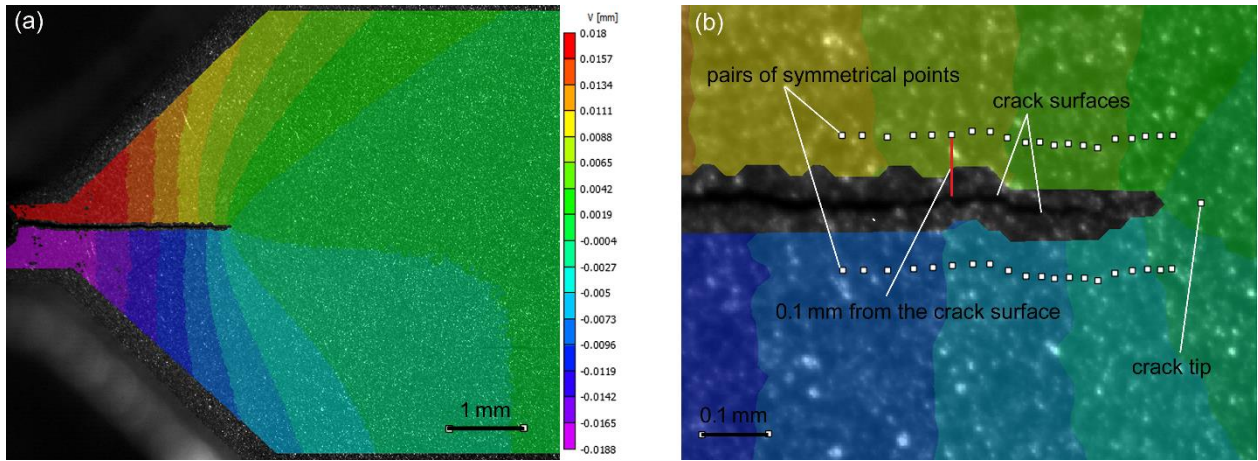


Figure 5 (a) Vertical displacement map from DIC analysis corresponding to $K_{\max} = 29.8 \text{ MPa}\sqrt{\text{m}}$. (b) pairs of symmetrical points along the crack flanks to obtain CTOD measurements.

The plastic component of the CTOD is then extracted from CTOD curves of each pair of symmetrical points through mathematical processing of the data following the procedure described in Figure 1. The methodology was implemented in a Matlab program that allows computing the total ΔCTOD_p values. The results of this analysis for two different crack extensions as shown in Figure 6. It can be observed that the amount of plastic deformation measured by CTOD_p increases with increasing crack length from 6 to 8 mm. Moreover, the ΔCTOD_p values are lower close to the crack tip and increase to their maximum value in the range location of approximately $100 - 150 \mu\text{m}$ behind the crack tip. This result is in agreement with the sensitivity analysis process performed by Vasco et al. [32-33] to identify the suitable location to obtain CTOD_p measurements. Therefore, the maximum value for the corresponding crack length was stored.

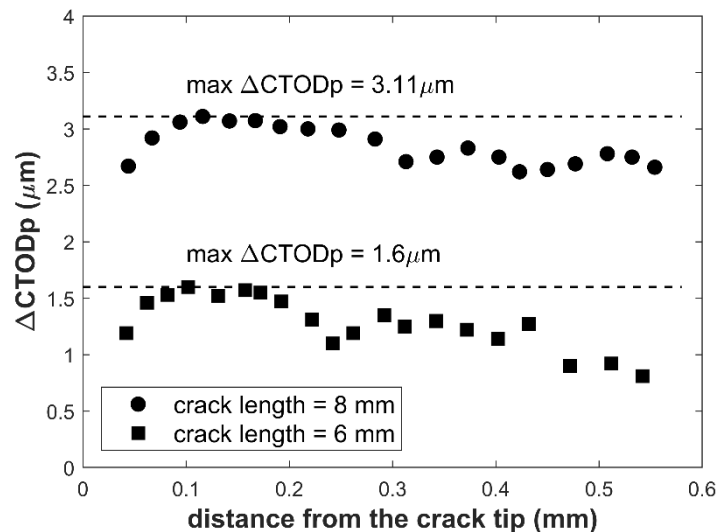


Figure 6. ΔCTOD_p values along the crack surface for crack lengths of 6 mm and 8 mm.

3. Experimental results

1
2
3
4
5
6
7
8
9
10
11
12
13
14
15
16
17
18
19
20
21
22
23
24
25
26
27
28
29
30
31
32
33
34
35
36
37
38
39
40
41
42
43
44
45
46
47
48
49
50
51
52
53
54
55
56
57
58
59
60
61
62
63
64
65

The experimental values of da/dN calculated versus the crack lengths from FCG tests for samples without and with overload application are shown in Figures 7a and 7b, respectively. From the experimental data, it can be seen that, before the OL application, the sample with OL shows similar behavior to the sample without OL. The da/dN values increase with the ΔK associated with the actual crack size and, the imposition of a 50% overload cycle leads to a period of retardation in crack propagation, decreasing the FCG rate. It is worth emphasizing that in ductile materials, a single-cycle overload may lead to crack blunting by the plastic deformation that takes place at the crack tip. Crack blunting keeps the tip opened, eliminating crack closure effects [39]. As a result, before the crack retardation begins, a very short acceleration in FCG rates may be observed right after its application. The acceleration event is usually observed when the overload ratio ($R_{OL}=F_{OL}/F_{max}$) is greater than 1.5 [40]. In this experiment, crack growth acceleration was observed immediately after OL within a crack length increment of 0.05 mm from its application.

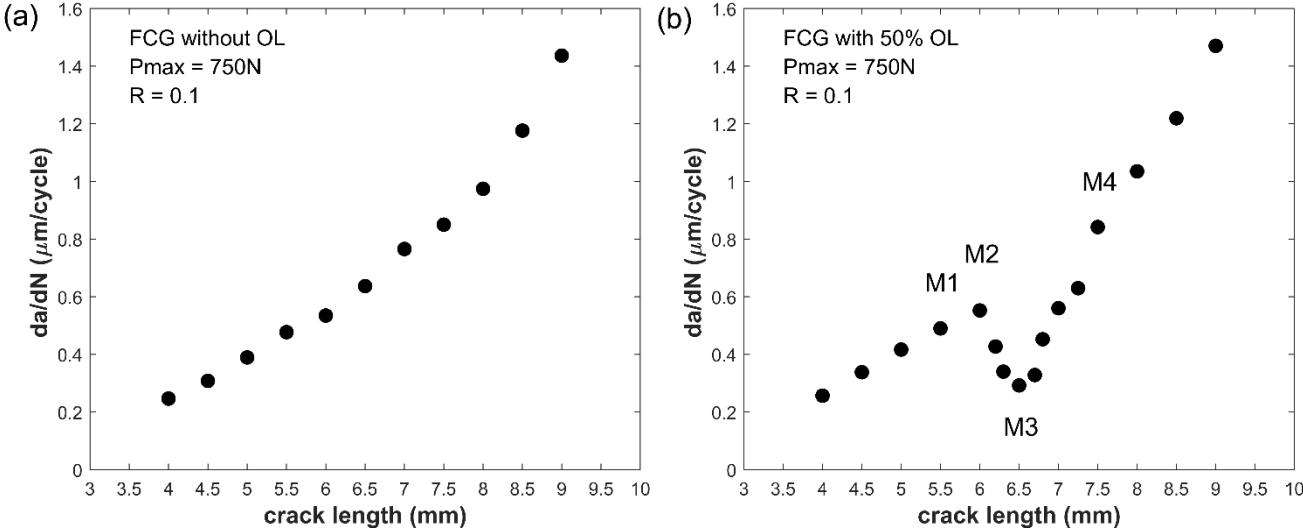


Figure 7. Crack growth rates vs crack length for samples without (a) and with (b) overload event.

Crack-tip opening displacement (CTOD) measurements at different crack lengths were taken to assess the effect of the overload application in the crack opening-closing mechanism. The analyzed points are shown in Figure 7b: points M1 and M2, before the OL application, represent crack lengths of 5.5 and 6 mm, respectively, the maximum retardation in growth rates occurs at point M3, which corresponds to a crack length of 6.5 mm, and lastly, the crack at point M4 has a length of 7.5 mm and is outside the OL-induced retardation zone. The results of this analysis are shown in Figure 8 corresponding to CTOD measurements obtained at 1 mm behind the crack tip. It can be seen that these curves exhibit similar behavior to the total CTOD curve presented in Figure 1 based on numerical predictions extracted from the first node at 8 μm behind the crack tip. Therefore, there is a portion of the CTOD curve corresponding to the unzipping of

crack flanks from the measurement point to the crack tip. This region is identified in Figure 8b from the minimum loading to a load of approximately 166 N, marked with a square. The slope that describes the elastic behavior of the material must be identified in the unloading portion of the curve, as indicated in Figure 8b. The translation of the curve to the loading part of the curve can be used to define the point marked with the square at which the crack is considered completely open. The same procedure was made in all CTOD measurements. It can be observed that the range of CTOD increases from M1 (see Figure 8a) to M2 (see Figure 8b) according to the increasing length of the crack. A small increase in elastic and plastic CTOD ranges is therefore expected. The crack opening levels are similar, i.e. $U^* = 17\%$ where U^* is the portion of the load cycle in which the crack surface is closed:

$$U^* = \frac{F_{open} - F_{min}}{F_{max} - F_{min}} \times 100 \quad (1)$$

where F_{open} is the crack opening load, and F_{min} and F_{max} are the minimum and maximum loads, respectively.

It can be observed that the crack opening level from the CTOD curve at the minimum FCG rate (point M3 in Figure 8c) is significantly higher $U^* = 43\%$, reducing the elastic and plastic CTOD ranges. According to the PICC model, as the crack propagated into the material following the overload, the greater response of the residual elastic ligaments over the plastic zones perturbed by the overload tends to compress it. This behavior reduces the crack opening-closing mechanism since a portion of the applied load is devoted to relieving the compressive loads transmitted through its faces as shown in CTOD curves of Figure 8c. Lastly, the CTOD curve at M4 (Figure 8d) exhibits similar behavior to the curves at M1 and M2, with low crack closure levels ($U^* = 19\%$). Relatively to M2, there is a significant increase in total CTOD, and consequently in plastic and elastic CTOD ranges. This increase in CTOD is explained by the effect of crack length on displacement fields. These experimental results indicated that the change in FCG rate produced by the imposition of the 50% overload is linked to the crack opening-closing mechanism. According to the literature, the effects of a single peak overload cycle are predominately due to residual stresses emerging in front of the crack tip [40], plasticity-induced crack closure acting on the crack surfaces behind the crack tip, or a combination of both. This phenomenon was recently studied by Borges et al. [12] through numerical simulations, verifying that the effect of overloads in FCG is mainly explained by plasticity-induced crack closure.

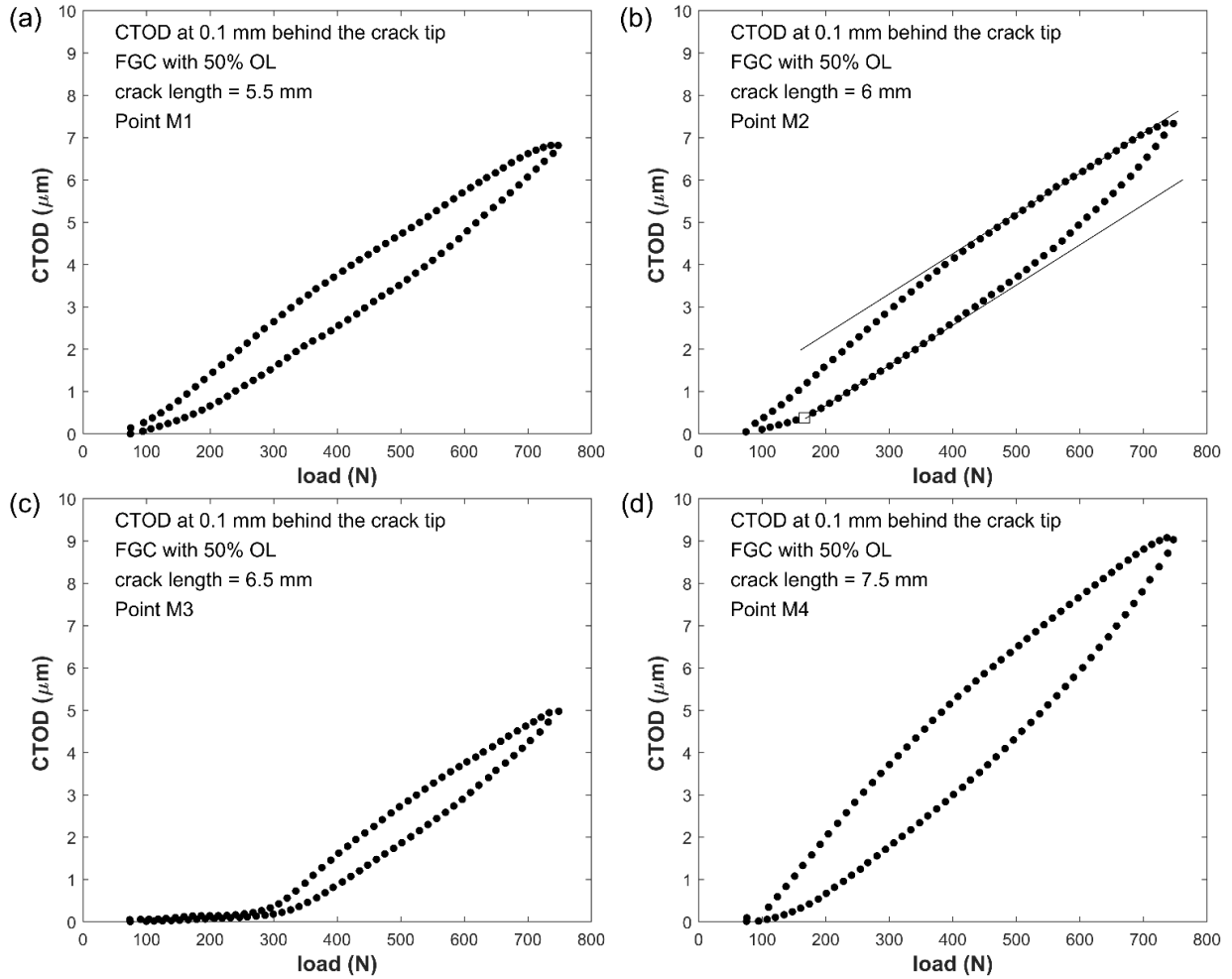


Figure 8. CTOD measurements by DIC analysis at different crack lengths for the sample with OL event: crack lengths of (a) 5.5 mm, (b) 6 mm, (c) 6.5 mm, and (d) 7.5 mm.

In the next analysis step, the methodology described in the previous section was applied to obtain the $CTOD_p$ from the experimental data recorded from samples without and with overload events. Then, the plastic CTOD ranges were plotted versus the crack growth rates (da/dN) plotted in linear scales as shown in Figure 9. It can be seen that the relation $\Delta CTOD_p$ - da/dN obtained from the FCG with OL application follows a linear trend (see Figure 9b), similar to the non-OL case (see Figure 9a), taking into account the load sequence effects due to the imposed OL. As shown in Figure 9b, after the OL application at P1, the da/dN values begin to decrease following the linear trend depicted before the OL, and after reaching its minimum value at P2, da/dN values begin to increase following the same trend. The linear relationships for the crack growth rates of these fatigue tests are given by the following equations:

$$\frac{da}{dN} = 0.317 \times \Delta CTOD_p \quad (\text{without overload}) \quad (2)$$

$$\frac{da}{dN} = 0.338 \times \Delta CTOD_p \quad (\text{with overload}) \quad (3)$$

As expected, the constant α from equations 2 and 3 are very similar, showing that the equation $da/dN = \alpha \times \Delta CTOD_p$ takes into account the load sequence effects due to the imposed OL. Moreover, it is worth mentioning that both values of α are also in agreement with those obtained in previous work [32] conducted on the same material. Therefore, the constant α can be treated as an intrinsic property of the material. The small differences observed between them can be associated with the inherent scattering from experimental data and the methodology used to obtain the $CTOD_p$.

From these experimental results, despite the load sequence effects regarding the overload application, the $CTOD_p$ parameter has demonstrated a consistent correlation with crack growth rates. Moreover, its application is interesting because it allows for establishing a linear relationship with FCG rates in linear scales, independent of loading conditions.

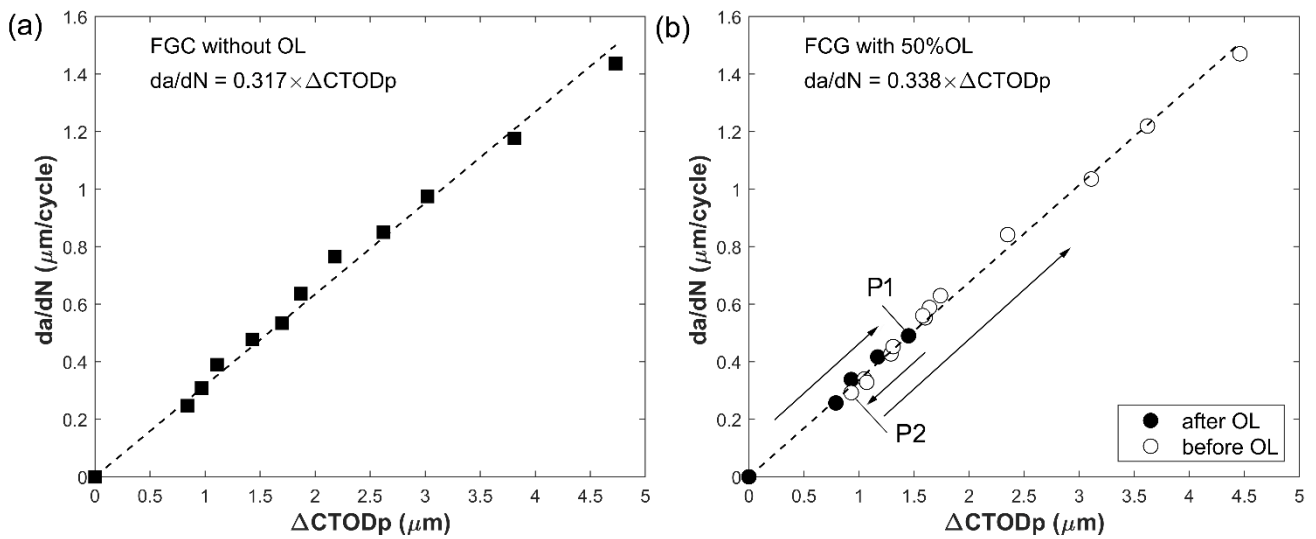


Figure 9. Plots of da/dN - $CTOD_p$ relationships for the two FCG tests (a) without and (b) with overload application.

Finally, the experimental data shown in Figure 10 is clear evidence of the good agreement between the $CTOD_p$ and the variations in FCG rates. It can be seen that the application of the 50% overload resulted in a transient effect that persisted for some extent until the crack grows beyond the region of influence caused by the overload. In fact, the minimum crack growth rate was registered after the crack grows for a period after the OL application, a phenomenon called delayed retardation that was correctly modeled by the $CTOD_p$. After reaching the maximum retardation, FCG rates begin to increase gradually and nonlinearly following typical retardation response for the plane stress case. The good correspondence between the FCG rates and $\Delta CTOD_p$ during the post-overload behavior is quite interesting because it

demonstrates that the $CTOD_p$ takes into account the mechanisms and related phenomena acting on the crack growth after the overload application.

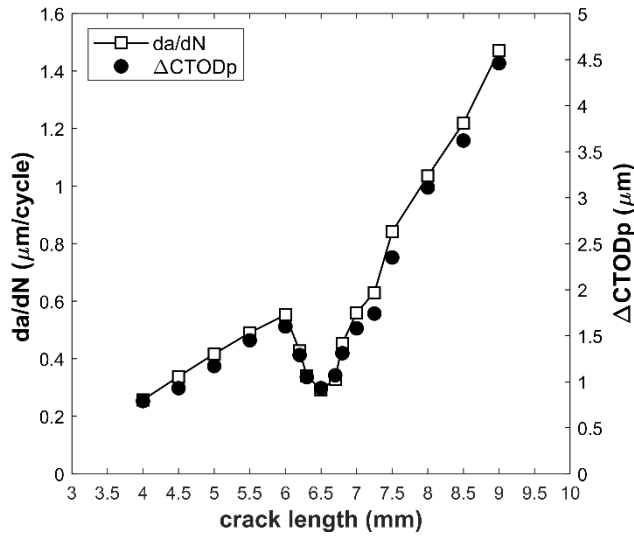


Figure 10. Plots of the da/dN and $\Delta CTOD_p$ versus crack length.

In order to visualize the effects of cycle interaction by the imposition of the single 50% OL, the variation of the crack-tip plastic zone during the post-overload propagation was characterized following the methods outlined in previous studies [41, 42]. From the experimental results presented in Figure 11a the following observations are made: (a) As expected, the OL induced an increase in the monotonic plastic zone size. (b) As the crack propagates inside the overload plastic zone, the interaction of the current plastic zone with the region perturbed by the overload can be observed, decreasing its size after OL application to maximum retardation reported at position OL+0.5 mm and increasing its size when getting away from this area. (c) It is clear that after reaching the maximum retardation, the size of the successive plastic zones increases as the crack leaves the region perturbed by the OL. (d) The extent of the overload plastic zone right of the crack tip is about 0.89 mm while positions OL+1 mm and OL+1.25 mm in the da/dN curve still indicate OL-induced effects acting in this region, as shown in Figure 11b. This could be expected because the crack closure phenomenon results from the residual plastic wake, so the crack tip must move some distance ahead of the region hypertrophied by the OL to disappear all its effects. It can be noted that all these cycle interaction effects were properly taken into account by the $CTOD_p$ following the linear relationship described by equation 3.

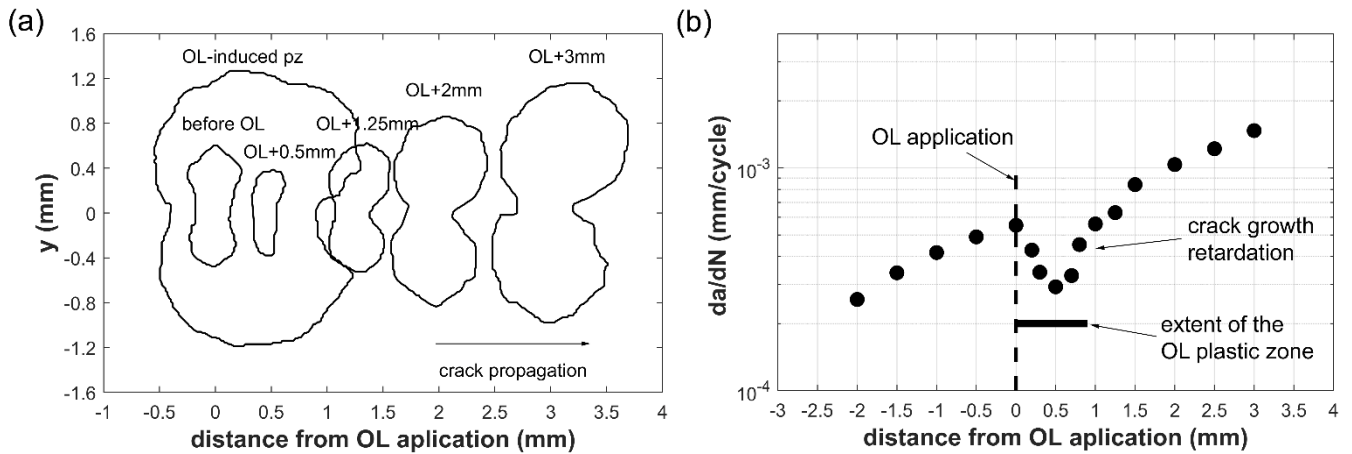


Figure 11. (a) Evolution of the plastic zone during the post-overload crack propagation. (b) FCG rates in logarithmic scale versus crack growth increment.

4. Discussion

The analysis of CTOD proved to be very useful because it can be used as a sensor of crack tip phenomena, namely, crack opening and closing, elastic deformation, and plastic deformation. The plastic deformation is quantified by subtracting the elastic component from the total CTOD, with its maximum value, $\Delta CTOD_p$, quantified at the maximum load. It is essential to emphasize that this parameter includes the effects of crack closure induced by plasticity, crack tip blunting, and residual stresses which are relevant in FCG under variable amplitude loading. In addition, the plastic CTOD has demonstrated a linear correlation with da/dN . This suggests that the primary damage mechanism responsible for FCG in Grade 2 titanium is crack-tip plastic deformation. The same conclusion was obtained in numerical and experimental studies. Neto et al. [43] found a good agreement between numerical predictions and experimental results obtained for MT specimens made of 6082-T6 aluminum alloy submitted to load blocks. Leitner et al. [44] examined nickel samples with grain sizes in the microcrystalline to the nanocrystalline range. In the near-threshold region up to the Paris regime, dislocation motion is the predominant damage mechanism, regardless of grain size, according to FCG measurements for various load ratios and extensive fracture surface analyses.

The linearity of da/dN versus $\Delta CTOD_p$ relation has been also observed in experimental results reported in previous studies for other materials, as shown in Figure 12. Therefore, the association between crack tip plastic deformation and FCG also occurs for other metallic materials. The variation of the α parameter of $da/dN = \alpha \times \Delta CTOD_p$ equation indicates that the same crack tip plastic deformation produces different crack extensions, depending on the material microstructure. Therefore, these results also suggest that the α parameter can be considered as an intrinsic material property.

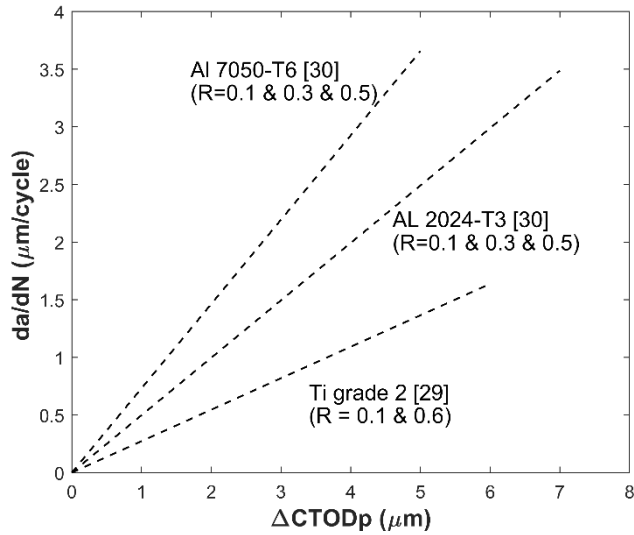


Figure 12. ΔCTOD_p vs da/dN curves for different materials from previous studies.

Finally, the mean stress effects in the ΔCTOD_p vs da/dN curves were also examined in this study by testing a sample with a different R-value. Figure 13 shows the results for an FCG conducted at $R = 0.3$. It can be observed that plotted data follows the same trend that the linear relationship previously defined for the material at $R = 0.1$. The fact that the crack closure is naturally included by the ΔCTOD_p parameter explains these experimental observations. Note that other phenomena, like partial closure, crack tip blunting, or damage below crack closure are also included in ΔCTOD_p . The ability to accommodate the effect of stress ratio has been widely used to validate crack driving parameters [45].

A recent paper [46] studied the variation of ΔK_{eff} and ΔCTOD_p along 3D curved crack fronts. The authors found equalized crack driving forces in terms of plastic CTOD along the crack front, which reinforces the ability of CTOD_p in the analysis of FCG.

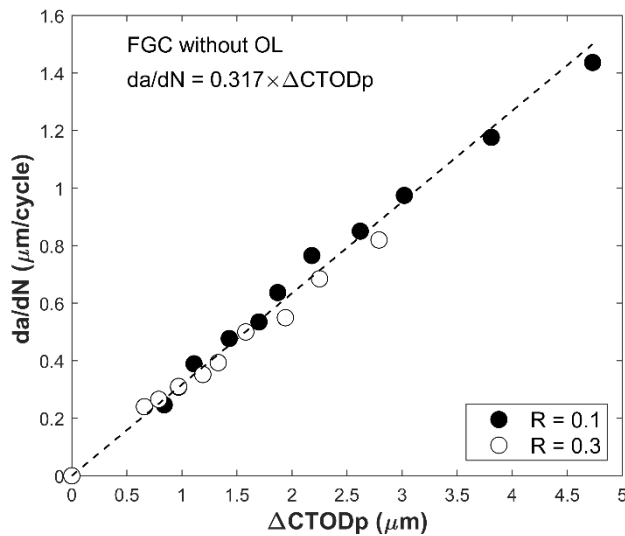


Figure 13. Plots of da/dN - ΔCTOD_p for tests conducted at different stress ratio values

5. Conclusions

An experimental study was conducted to examine the reliability of the viable use of plastic crack-tip opening displacement ($CTOD_p$) as a crack driving parameter for fatigue crack growth in a Grade 2 titanium sample following a single tensile overload. The main conclusions are:

- From the experimental results, the direct proportionality of the $\Delta CTOD_p$ vs da/dN curve was verified. It can be concluded that, for the test condition investigated, the OL-induced FCG retardation and related phenomena were naturally included in $\Delta CTOD_p$ measurements, prevailing the linear correspondence with fatigue crack growth rates.

It is worth emphasizing that $CTOD_p$ is a parameter, directly measured from the test, which establishes a link with the plastic deformation developed in front of the crack tip where the crack propagation occurs. Furthermore, it can be concluded that the primary damage mechanism responsible for FCG tests in Grade 2 titanium was the crack tip plastic deformation.

- The α parameter of $da/dN = \alpha \times \Delta CTOD_p$ relation changes with material, therefore it can be considered an intrinsic material property. In fact, the increase of the α parameter indicates that the same crack tip plastic deformation produces larger crack extensions, and this depends on the material microstructure.

- The $da/dN = \alpha \times \Delta CTOD_p$ relation is also independent of stress ratio in constant amplitude tests.

Therefore, these experimental results suggest the feasible use of the $CTOD_p$ as a driving force parameter for fatigue crack growth. In the future, it will be important to establish links between the α parameter and material microstructure. In fact, the α parameter quantifies the efficiency of crack tip plastic deformation in the production of crack growth, which is expected to be greatly dependent on microstructure. Additionally, it will be interesting to compare DIC measurements of plastic CTOD with numerical predictions obtained for plane stress and plane strain states, which is important for a better understanding of the effect of thickness on surface measurements.

Acknowledgments

The authors would like to acknowledge the financial support from Ministerio de Universidades del Gobierno de España through the program “Recualificación del Sistema Universitario Español 2021-2023: ayudas Maria Zambrano”, the Junta de Andalucía through the research project “1380786” funded by the program “Proyectos de I + D + i en el Marco del Programa Operativo FEDER Andalucía 2014-2020, also the portuguese funds through FCT-Fundação para a Ciência e a Tecnologia –, under the project UIDB/00285/2020.

References

- [1] J.R. Rice, The mechanics of crack tip deformation and extension by fatigue, Division of Engineering, Brown University, 1966, <https://doi.org/10.1520/stp47234s>
- [2] W. Elber, The significance of fatigue crack closure, (1971), <https://doi.org/10.1520/stp26680s>
- [3] E. Von Euw, R. Hertzberg, R. Roberts, Delay effects in fatigue crack propagation, *Astm Stp*, 513 (1972) 230-259, <https://doi.org/10.1520/STP34123S>
- [4] C. Shin, N. Fleck, Overload retardation in a structural steel, *Fatigue & Fracture of Engineering Materials & Structures*, 9 (1987) 379-393, <https://doi.org/10.1111/j.1460-2695.1987.tb00464.x>
- [5] W. Mills, R. Hertzberg, The effect of sheet thickness on fatigue crack retardation in 2024-T3 aluminum alloy, *Engineering Fracture Mechanics*, 7 (1975) 705-711, [https://doi.org/10.1016/0013-7944\(75\)90026-0](https://doi.org/10.1016/0013-7944(75)90026-0)
- [6] C. Shin, S. Hsu, On the mechanisms and behaviour of overload retardation in AISI 304 stainless steel, *International Journal of Fatigue*, 15 (1993) 181-192, [https://doi.org/10.1016/0142-1123\(93\)90175-p](https://doi.org/10.1016/0142-1123(93)90175-p)
- [7] K. Sadananda, A. Vasudevan, R. Holtz, E. Lee, Analysis of overload effects and related phenomena, *International Journal of Fatigue*, 21 (1999) S233-S246, [https://doi.org/10.1016/s0142-1123\(99\)00094-8](https://doi.org/10.1016/s0142-1123(99)00094-8)
- [8] R. Pippan, A. Hohenwarter, Fatigue crack closure: a review of the physical phenomena, *Fatigue & fracture of engineering materials & structures*, 40 (2017) 471-495, <https://doi.org/10.1111/ffe.12578>
- [9] P. Paris, F. Erdogan, A critical analysis of crack propagation laws, (1963). <https://doi.org/10.1115/1.3656900>
- [10] D. Kujawski, Discussion and Comments on KOP and ΔK_{eff} , *Materials*, 2020, pp. 4959, <https://doi.org/10.3390/ma13214959>
- [11] M.F. Borges, D.M. Neto, F.V. Antunes, Revisiting classical issues of fatigue crack growth using a non-linear approach, *Materials*, 13 (2020) 5544, <https://doi.org/10.3390/ma13235544>
- [12] J.A.O. González, J.T.P. de Castro, M.A. Meggiolaro, G.L.G. Gonzáles, J.L. de Franca Freire, Challenging the “ ΔK_{eff} is the driving force for fatigue crack growth” hypothesis, *International Journal of Fatigue*, 136 (2020) 105577, <https://doi.org/10.1016/j.ijfatigue.2020.105577>
- [13] D. Kujawski, On assumptions associated with ΔK_{eff} and their implications on FCG predictions, *International journal of fatigue*, 27 (2005) 1267-1276, <https://doi.org/10.1016/j.ijfatigue.2005.07.020>
- [14] K. Sadananda, D.-N.V. Ramaswamy, Role of crack tip plasticity in fatigue crack growth, *Philosophical Magazine A*, 81 (2001) 1283-1303, <https://doi.org/10.1080/01418610108214441>
- [15] F. Antunes, T. Sousa, R. Branco, L. Correia, Effect of crack closure on non-linear crack tip parameters, *International Journal of Fatigue*, 71 (2015) 53-63, <https://doi.org/10.1016/j.ijfatigue.2014.10.001>
- [16] J. Pokluda, Dislocation-based model of plasticity and roughness-induced crack closure, *International journal of fatigue*, 46 (2013) 35-40, <https://doi.org/10.1016/j.ijfatigue.2011.11.016>

- 1 [17] H. Chen, W. Chen, T. Li, J. Ure, Effect of circular holes on the ratchet limit and crack tip plastic strain range in
2 a centre cracked plate, *Engineering fracture mechanics*, 78 (2011) 2310-2324,
3 <https://doi.org/10.1016/j.engfracmech.2011.05.004>
4
- 5 [18] H.-B. Park, K.-M. Kim, B.-W. Lee, Plastic zone size in fatigue cracking, *International journal of pressure*
6 *vessels and piping*, 68 (1996) 279-285, [https://doi.org/10.1016/0308-0161\(95\)00066-6](https://doi.org/10.1016/0308-0161(95)00066-6)
7
- 8 [19] J.-Z. Zhang, J.-Z. Zhang, S.Y. Du, Elastic-plastic finite element analysis and experimental study of short and
9 long fatigue crack growth, *Engineering Fracture Mechanics*, 68 (2001) 1591-1605,
10 [https://doi.org/10.1016/s0013-7944\(01\)00047-9](https://doi.org/10.1016/s0013-7944(01)00047-9)
11
- 12 [20] S. Bodner, D. Davidson, J. Lankford, A description of fatigue crack growth in terms of plastic work,
13 *Engineering Fracture Mechanics*, 17 (1983) 189-191, [https://doi.org/10.1016/0013-7944\(83\)90169-8](https://doi.org/10.1016/0013-7944(83)90169-8)
14
- 15 [21] N.W. Klingbeil, A total dissipated energy theory of fatigue crack growth in ductile solids, *International*
16 *Journal of Fatigue*, 25 (2003) 117-128, [https://doi.org/10.1016/s0142-1123\(02\)00073-7](https://doi.org/10.1016/s0142-1123(02)00073-7)
17
- 18 [22] L. Campbell. The influence of metallurgical structure on the mechanisms of fatigue crack propagation. *ASTM*
19 *STP 415 (1967): 131-168*, <https://doi.org/10.1520/STP47230S>
20
- 21 [23] R. N. Pelloux. Crack extension by alternating shear. *Engineering Fracture Mechanics*, 1 (1970), 697-704,
22 [https://doi.org/10.1016/0013-7944\(70\)90008-1](https://doi.org/10.1016/0013-7944(70)90008-1).
23
- 24 [24] P. Neumann. The geometry of slip processes at a propagating fatigue crack—II. *Acta Metallurgica* 22.9
25 (1974): 1167-1178, [https://doi.org/10.1016/0001-6160\(74\)90072-8](https://doi.org/10.1016/0001-6160(74)90072-8)
26
- 27 [25] V. Tvergaard, On fatigue crack growth in ductile materials by crack-tip blunting, *Journal of the Mechanics*
28 *and Physics of Solids*, 52 (2004) 2149-2166, <https://doi.org/10.1016/j.jmps.2004.02.007>
29
- 30 [26] R. Pippan, W. Grosinger, Fatigue crack closure: From LCF to small scale yielding, *International journal of*
31 *fatigue*, 46 (2013) 41-48, <https://doi.org/10.1016/j.ijfatigue.2012.02.016>
32
- 33 [27] W. Guo, C. Wang, L. Rose, The influence of cross-sectional thickness on fatigue crack growth, *Fatigue &*
34 *Fracture of Engineering Materials & Structures*, 22 (1999) 437-444, <https://doi.org/10.1046/j.1460-2695.1999.00176.x>
35
- 36 [28] A. Ktari, M. Baccar, M. Shah, N. Haddar, H. Ayedi, F. Rezai-Aria, A crack propagation criterion based on
37 Δ CTOD measured with 2D-digital image correlation technique, *Fatigue & Fracture of Engineering Materials &*
38 *Structures*, 37 (2014) 682-694, <https://doi.org/10.1111/ffe.12153>
39
- 40 [29] A. Shahani, H.M. Kashani, M. Rastegar, M.B. Dehkordi, A unified model for the fatigue crack growth rate in
41 variable stress ratio, *Fatigue & Fracture of Engineering Materials & Structures*, 32 (2009) 105-118,
42 <https://doi.org/10.1111/j.1460-2695.2008.01315.x>
43
- 44 [30] F. Antunes, S. Rodrigues, R. Branco, D. Camas, A numerical analysis of CTOD in constant amplitude fatigue
45 crack growth, *Theoretical and Applied Fracture Mechanics*, 85 (2016) 45-55,
46 <https://doi.org/10.1016/j.tafmec.2016.08.015>
47
- 48
49
50
51
52
53
54
55
56
57
58
59
60
61
62
63
64
65

- 1 [31] F. Antunes, R. Branco, P. Prates, L. Borrego, Fatigue crack growth modelling based on CTOD for the 7050-T6
2 alloy, *Fatigue & Fracture of Engineering Materials & Structures*, 40 (2017) 1309-1320,
3 <https://doi.org/10.1111/ffe.12582>
4
- 5 [32] J. Vasco-Olmo, F. Díaz, F. Antunes, M. James, Characterisation of fatigue crack growth using digital image
6 correlation measurements of plastic CTOD, *Theoretical and Applied Fracture Mechanics*, 101 (2019) 332-341,
7 <https://doi.org/10.1016/j.tafmec.2019.03.009>
8
- 9 [33] J.M. Vasco-Olmo, F.A. Diaz Garrido, F.V. Antunes, M. James, Plastic CTOD as fatigue crack growth
10 characterising parameter in 2024-T3 and 7050-T6 aluminium alloys using DIC, *Fatigue & Fracture of Engineering*
11 *Materials & Structures*, 43 (2020) 1719-1730, <https://doi.org/10.1111/ffe.13210>
12
- 13 [34] G.L. Gonzales, J.A. Gonzalez, J.L. Freire, Characterization of discontinuous crack closure behavior after the
14 application of a single overload cycle, *Theoretical and Applied Fracture Mechanics*, 114 (2021) 103028,
15 <https://doi.org/10.1016/j.tafmec.2021.103028>
16
- 17 [35] D. Nowell, P. De Matos, Application of digital image correlation to the investigation of crack closure
18 following overloads, *Procedia Engineering*, 2 (2010) 1035-1043, <https://doi.org/10.1016/j.proeng.2010.03.112>
19
- 20 [36] Gonzáles, G. L. G., González, J. A. O., Castro, J. T. P., & Freire, J. L. F. Detecting fatigue crack closure and
21 crack growth delays after an overload using DIC measurements. In *Fracture, Fatigue, Failure and Damage*
22 *Evolution, Volume 7: Proceedings of the 2017 Annual Conference on Experimental and Applied Mechanics*,
23 Springer International Publishing. (2018) pp. 57-65, https://doi.org/10.1007/978-3-319-62831-8_8
24
- 25 [37] Gonzáles, G. L. G., González, J. A. O., Neto, D. M., Antunes, F. V., & Díaz, F. A. Experimental determination of
26 the reversed plastic zone size around fatigue crack using Digital Image Correlation. *Theoretical and Applied*
27 *Fracture Mechanics*, (2023) 103901, <https://doi.org/10.1016/j.tafmec.2023.103901>
28
- 29 [38] International Digital Image Correlation Society, Jones, E.M.C. and Iadicola, M.A. (Eds.) (2018). A Good
30 Practices Guide for Digital Image Correlation, <https://doi.org/10.32720/idics/gpg.ed1/print.format>.
31
- 32 [39] G. Gonzáles, J. Diaz, J. González, J. Castro, J.d.F. Freire, Determining SIFs using DIC considering crack closure
33 and blunting, in: *Experimental and Applied Mechanics, Volume 4*, Springer, 2017, pp. 25-36,
34 https://doi.org/10.1007/978-3-319-42028-8_4
35
- 36 [40] E. Salvati, S. O'connor, T. Sui, D. Nowell, A. Korsunsky, A study of overload effect on fatigue crack
37 propagation using EBSD, FIB–DIC and FEM methods, *Engineering Fracture Mechanics*, 167 (2016) 210-223,
38 <https://doi.org/10.1016/j.engfracmech.2016.04.034>
39
- 40 [41] J. Vasco-Olmo, M. James, C. Christopher, E. Patterson, F. Díaz, Assessment of crack tip plastic zone size and
41 shape and its influence on crack tip shielding, *Fatigue & Fracture of Engineering Materials & Structures*, 39
42 (2016) 969-981, <https://doi.org/10.1111/ffe.12436>
43
- 44 [42] G. Gonzáles, J. González, V. Paiva, J. Freire, Crack-tip plastic zone size and shape via DIC, in: *Fracture,*
45 *Fatigue, Failure and Damage Evolution, Volume 6*, Springer, 2019, pp. 5-10, https://doi.org/10.1007/978-3-319-95879-8_2
46
47
48
49
50
51
52
53
54
55
56
57
58
59
60
61
62
63
64
65

1
2
3
4
5
6
7
8
9
10
11
12
13
14
15
16
17
18
19
20
21
22
23
24
25
26
27
28
29
30
31
32
33
34
35
36
37
38
39
40
41
42
43
44
45
46
47
48
49
50
51
52
53
54
55
56
57
58
59
60
61
62
63
64
65

[43] D. Neto, E. Sérgio, M. Borges, L. Borrego, F. Antunes, Effect of load blocks on fatigue crack growth, International Journal of Fatigue, 162 (2022) 107001, <https://doi.org/10.1016/j.ijfatigue.2022.107001>

[44] T. Leitner, A. Hohenwarter, R. Pippan, Revisiting fatigue crack growth in various grain size regimes of Ni, Materials Science and Engineering: A, 646 (2015) 294-305, <https://doi.org/10.1016/j.msea.2015.08.071>

[45] Daniel Kujawski, A fatigue crack driving force parameter with load ratio effects, International Journal of Fatigue 23 (2001) S239–S246, [https://doi.org/10.1016/S0142-1123\(01\)00158-X](https://doi.org/10.1016/S0142-1123(01)00158-X)

[46] T. Oplt, T. Vojtek, R. Kubíček, P. Pokorný, P. Hutař, Numerical modelling of fatigue crack closure and its implication on crack front curvature using $\Delta CTOD_p$, International Journal of Fatigue, (2023) 107570, <https://doi.org/10.1016/j.ijfatigue.2023.107570>

Declaration of interests

The authors declare that they have no known competing financial interests or personal relationships that could have appeared to influence the work reported in this paper.

The authors declare the following financial interests/personal relationships which may be considered as potential competing interests:

Experimental analysis of the plastic CTOD to characterize the variable amplitude fatigue crack growth in Grade 2 titanium samples

Giancarlo L. Gómez Gonzales^a, Jose M. Vasco-Olmo^a, Fernando V. Antunes^b, Diogo M. Neto^b, Francisco A. Díaz^a

^aDepartamento de Ingeniería Mecánica y Minera, University of Jaén, Jaén, Spain.

^bDepartment of Mechanical Engineering, Centre for Mechanical Engineering, Materials and Processes (CEMMPRE), University of Coimbra, Coimbra, Portugal.

Abstract

In this paper, the plastic component of the crack-tip opening displacement (CTOD_p) is experimentally evaluated to characterize the fatigue crack growth behavior in a Grade 2 titanium sample under single overload with constant amplitude loading conditions. The CTOD measurements were performed with the 2D-Digital Image Correlation (DIC) technique. The experimental results show a linear correlation between CTOD_p and fatigue crack growth rates, suggesting the independence of this relationship to load-interaction effects. Therefore, this study demonstrates that the CTOD_p can be a suitable crack-driving parameter to study crack propagation behavior under variable amplitude loading. Furthermore, it suggests that the fatigue crack growth process is primarily caused by cyclic plastic deformation.

Keywords: Fatigue crack growth, grade 2 titanium, overload, DIC, CTOD

Nomenclature

2D	bidimensional dimension
CT	compact tension
CTOD	crack tip opening displacement
CTOD _p	plastic CTOD
E	Young's modulus
F	applied force
FCG	fatigue crack growth
K	stress intensity factor
OL	overload
PICC	plastic-induced crack closure
R	load ratio
U*	crack closure level
v	vertical displacement
α	numeric constant
ΔCTOD _p	range of plastic CTOD
ΔK	stress intensity factor range

ΔK_{eff}	effective stress intensity factor range
$\Delta \varepsilon$	strain range
$\Delta \sigma$	stress range
ε	strain
$\varepsilon_y, \varepsilon_{cy}$	yield strain, cyclic yield strain
σ	stress
σ_y, σ_{cy}	yield stress, cyclic yield stress

1. Introduction

Despite the numerous studies [1-8] devoted to understanding the phenomenon of fatigue crack growth (FCG) under different loading conditions, the prediction of fatigue life in real engineering structures with crack-like defects remains challenging. This results from the difficulty of developing a universal equation to describe the load sequence effects taking into account all the complex mechanisms involved in the FCG process. This concerns, for example, plasticity-induced crack closure (PICC), crack roughness, crack closure induced by corrosion, residual stresses, crack blunting and crack branching, among others.

Although the small-scale cyclic plasticity at the crack tip due to cyclic loading can be successfully described with the stress intensity factor range, ΔK , the FCG rates (da/dN) vs ΔK relation proposed by Paris and Erdogan [9] does not account for mean stress effects (described by the R-ratio) and load-interaction or load-history effects. In fact, Paris's law is often used to assess experimental FCG rates vs ΔK data from constant amplitude loading fatigue tests whereas real engineering components are commonly submitted to non-uniform loading. Instead of using the ΔK , Elber [2] proposed the effective stress intensity factor range, ΔK_{eff} , which is affected by crack closure under a certain load level, i.e. $\Delta K_{\text{eff}} = K_{\text{max}} - K_{\text{open}}$ where K_{max} is the maximum stress intensity and K_{op} is the stress intensity at the crack opening. The crack closure concept became popular in literature since it can justify the effects of stress ratio and load history on fatigue crack propagation. However, it is still a topic of research and discussion within the fatigue community [10-14], as studies continue to be conducted to investigate the actual role of the crack closure mechanism in fatigue crack propagation.

In this context, non-linear parameters such as the CTOD_p, dissipated energy, J-integral, and plastic strain range have been suggested to correlate the crack-tip damage since they can effectively quantify the crack-tip plasticity. According to Antunes et al. [15], there are well-defined relationships between these parameters, as they all quantify the same phenomenon: the crack tip plastic deformation which is believed to be the main mechanism of fatigue crack growth. Nowadays, improved experimental techniques and numerical methods have made it possible to examine the near-tip region more closely, where the non-linear fatigue damage effectively occurs. Pokluda et al. [16] and Chen et al. [17] proposed the use of the

cyclic plastic strain range. Heung et al. [18] linked FCG with the cyclic plastic zone size, while Zhang et al. [19] conducted a numerical analysis, concluding that FCG can be correlated with the size of the monotonic plastic zone. Bodner et al. [20] and Klingbeil et al. [21] used the total dissipated energy as the crack driving force parameter to describe fatigue crack growth in ductile solids. In particular, the CTOD is an important fracture mechanics parameter used to characterize the local crack opening and closing, proving a physical meaning to the progressive crack extension under cyclic loading that occurs in yielding materials. The proportional relationship of the cyclic CTOD with the crack propagation rate (i.e. da/dN) has been proposed and experimentally and numerically investigated in a large number of papers, e.g. [22-29].

The significance of the plastic component of the CTOD ($CTOD_p$) was studied by Antunes et al. [30] through numerical experiments, showing its linear relationship with FCG rates in linear scales. They concluded that using the da/dN - $CTOD_p$ relation, the crack closure phenomenon, crack tip blunting, residual stresses, and fatigue threshold are included naturally. Furthermore, the independence of the da/dN - $CTOD_p$ relationship to the stress ratio for FCG tests was also verified by Antunes et al. [31] and Vasco et al. [32, 33] using FCG tests performed on aluminum and titanium specimens. In these studies, the CTOD measurements were obtained by DIC analysis, showing that only the plastic component on CTOD ($CTOD_p$) exhibits a consistent increase with FCG rates. These findings are equivalent to studies mentioned before in which the CTOD is measured directly at the crack tip, i.e. at a distance about CTOD behind the real blunted crack or at the position of the crack tip on the fracture surface of the last fatigue load cycle.

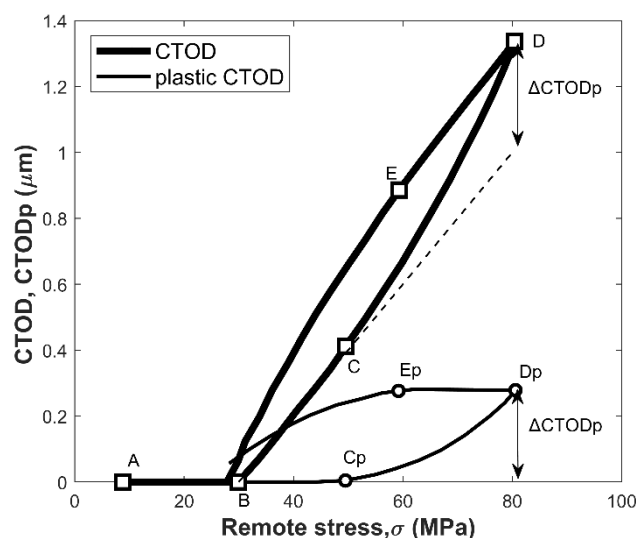


Figure 1. Variation of CTOD values throughout a full load cycle and determination of $CTOD_p$ [27].

Figure 1 shows the typical results obtained of total CTOD versus applied load from finite element simulation. Segment AB corresponds to the closed position of the crack. The crack opening and subsequent elastic behavior are observed in segment BC. As the loading is applied, plastic deformation is initiated during the segment CD. The value of the plastic CTOD ($CTOD_p$) is obtained after removing the elastic component from the total CTOD. For that, the extrapolation of the segment BC that corresponds to the elastic behavior of the material is required which is also parallel to the segment DE related to the elastic unloading. The evolution of plastic CTOD is also represented in Figure 1. $CTOD_p$ increases non-linearly from point C_p , which defines the end of the elastic regime, up to the maximum value registered at the maximum load (point D_p) defined by $\Delta CTOD_p$.

This paper follows the previous studies presented in Refs [31-33], exploring the applicability of the $CTOD_p$ parameter for the analysis of fatigue crack propagation after the application of a single overload (OL) during constant amplitude load. It is well known that one approach used to investigate the behavior of the mechanisms governing the FCG process consists in analyzing the effects caused by the imposition of simple load sequences such as single-cycle overload. The loading sequences can produce several load interaction effects, leading to acceleration or deceleration in fatigue crack growth rate. The significance of the non-linear parameters is that they can naturally accommodate the effects of load sequences, as well as stress state and specimen geometry, among others.

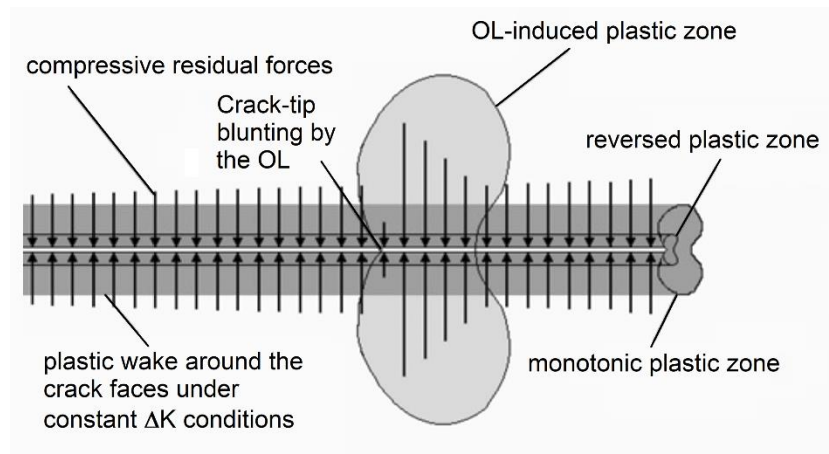


Figure 2. Scheme of Elber's OL-induced retardation.

It is well known that the imposition of a single peak overload retards the subsequent crack propagation for some period. Residual stresses ahead of the crack [7] and plasticity-induced crack closure acting on the crack surfaces [8] are identified as the main mechanisms for the crack retardation observed following overload application. As shown in the schematic of Figure 2, within the OL-induced plastic zone, larger residual stresses are generated which decrease from their maximum value to their initial value before the OL application. According to the PICC model, the effects caused by the OL event must cease after the

current plastic zone has left the region hypertrophied by the OL. However, studies [34,35] in the literature report OL-induced delay effects far away from the extension of the overload plastic zone, a phenomenon called discontinuous crack closure. Furthermore, crack propagation mechanisms may act concurrently or in competition, depending on a variety of factors like the crack extension, the material's microstructure, and the stress state, among others.

This investigation aims to study the fatigue crack behavior of Grade 2 titanium samples under overload conditions, and the feasible use of the $CTOD_p$ as a parameter for fatigue crack growth characterization. The CTOD measurements from the vertical displacement of the crack flanks, according to Mode-I (opening mode) were extracted using the 2D Digital Image Correlation (DIC) technique. Previous works [36, 37] reported its successful application to obtain CTOD measurements from multiscale experiments.

2. Experimental details

The FCG tests were conducted on a servo-hydraulic MTS testing machine (MTS machine with a load cell of 25 kN). The test samples were compact tension (CT) specimens machined from a 1mm thick sheet of Grade 2 titanium ($E = 105$ GPa and $\sigma_y = 390$ MPa). The specimen dimensions are provided in Figure 3a. The specimens were cycled at a cyclic frequency of 2 Hz under constant amplitude loading with a maximum level of 750 N and a stress ratio (R) of 0.1. Two samples were tested using the same loading conditions. In one of them, a single 50% tensile overload (i.e. a single cycle with a maximum loading of 1125 N) was applied manually after the crack reached a length of 6 mm (measured from the point of load application), and then constant amplitude loading was resumed (see Figure 3b).

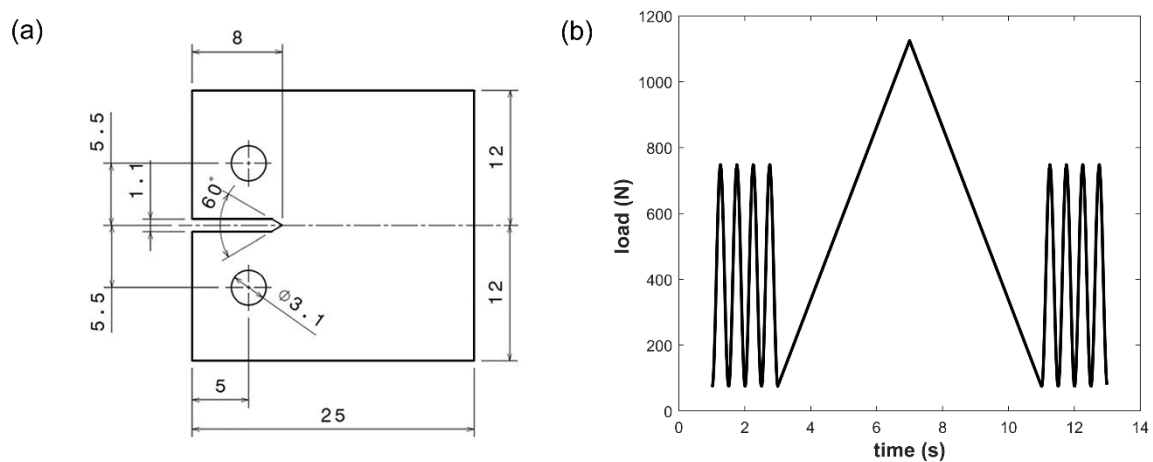


Figure 3. (a) Geometry of the sample (dimensions in mm), and (b) 2D-DIC setup used for investigation.

As mentioned earlier, the 2D-DIC analysis was adopted for investigation. For that, a high-resolution camera (Redwood 65MP sensor) coupled to high-magnification lenses (Laowa 60mm F2.8 2X) was located perpendicular to one face of the specimen. Besides, an additional camera (Stingray F-504B 5MP

sensor) was located in front of the other face to monitor the crack advance during the fatigue test, as shown in the experimental setup of Figure 4. During the FCG test, the cameras were configured to take about 100 images from each loading cycle analyzed. All images captured from FCG tests were processed with the commercial VIC-2D software from Correlated Solutions. The optical configuration achieves a spatial resolution of 2 $\mu\text{m}/\text{pixel}$. The displacement resolution estimated from an uncertainty assessment, also known as the noise floor [38], was 24 nm.

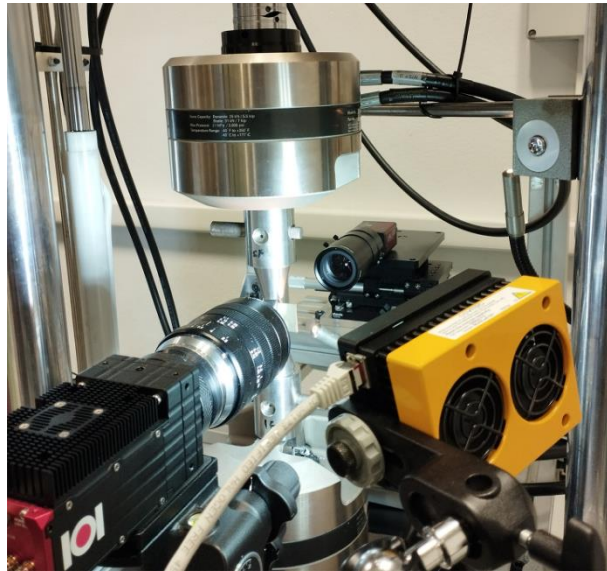


Figure 4. 2D-DIC setup used for investigation

2.1. Measurement of the plastic CTOD

Images of loading cycles captured at different crack lengths were processed by the DIC analysis software. In this analysis, the image registered at the minimum loading of each cycle was selected as the reference image. The DIC displacement maps, parallel to the load direction, were used to obtain the CTOD measurements according to Mode-I (opening mode).

The vertical displacement map provided by the DIC analysis at maximum loading for a crack length of 6 mm is depicted in Figure 5a. In this figure, the relative displacements are in agreement with the mode I of crack propagation or opening mode, in which the crack opens due to the application of stresses perpendicular to the plane in which it propagates. After the accurate localization of the crack tip, measurements of the crack opening–closing behavior are obtained by placing symmetrical points behind the crack tip at 0.1 mm from the flanks of the crack, as shown in Figure 5b. The relative displacement between the upper and lower crack flank is evaluated according to the following formula: $\text{CTOD} = v_{\text{upper}} - v_{\text{lower}}$, where v is the local measurement of the vertical displacement map.

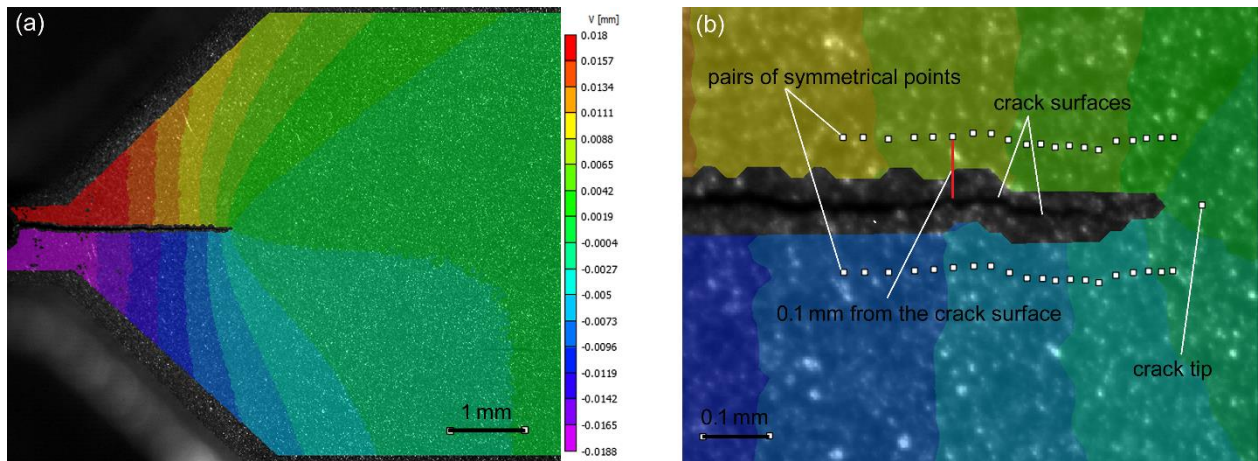


Figure 5 (a) Vertical displacement map from DIC analysis corresponding to $K_{\max} = 29.8 \text{ MPa}\sqrt{\text{m}}$. (b) pairs of symmetrical points along the crack flanks to obtain CTOD measurements.

The plastic component of the CTOD is then extracted from CTOD curves of each pair of symmetrical points through mathematical processing of the data following the procedure described in Figure 1. The methodology was implemented in a Matlab program that allows computing the total ΔCTOD_p values. The results of this analysis for two different crack extensions as shown in Figure 6. It can be observed that the amount of plastic deformation measured by CTOD_p increases with increasing crack length from 6 to 8 mm. Moreover, the ΔCTOD_p values are lower close to the crack tip and increase to their maximum value in the range location of approximately 100 – 150 μm behind the crack tip. This result is in agreement with the sensitivity analysis process performed by Vasco et al. [32-33] to identify the suitable location to obtain CTOD_p measurements. Therefore, the maximum value for the corresponding crack length was stored.

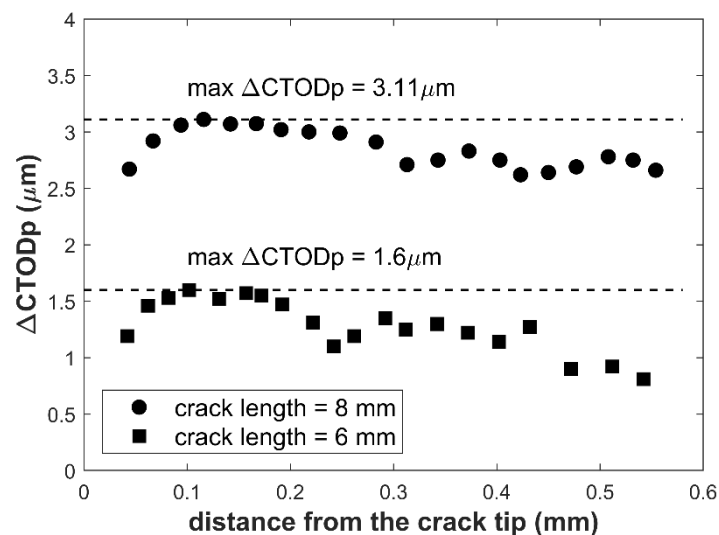


Figure 6. ΔCTOD_p values along the crack surface for crack lengths of 6 mm and 8 mm.

3. Experimental results

The experimental values of da/dN calculated versus the crack lengths from FCG tests for samples without and with overload application are shown in Figures 7a and 7b, respectively. From the experimental data, it can be seen that, before the OL application, the sample with OL shows similar behavior to the sample without OL. The da/dN values increase with the ΔK associated with the actual crack size and, the imposition of a 50% overload cycle leads to a period of retardation in crack propagation, decreasing the FCG rate. It is worth emphasizing that in ductile materials, a single-cycle overload may lead to crack blunting by the plastic deformation that takes place at the crack tip. Crack blunting keeps the tip opened, eliminating crack closure effects [39]. As a result, before the crack retardation begins, a very short acceleration in FCG rates may be observed right after its application. The acceleration event is usually observed when the overload ratio ($R_{OL}=F_{OL}/F_{max}$) is greater than 1.5 [40]. In this experiment, crack growth acceleration was observed immediately after OL within a crack length increment of 0.05 mm from its application.

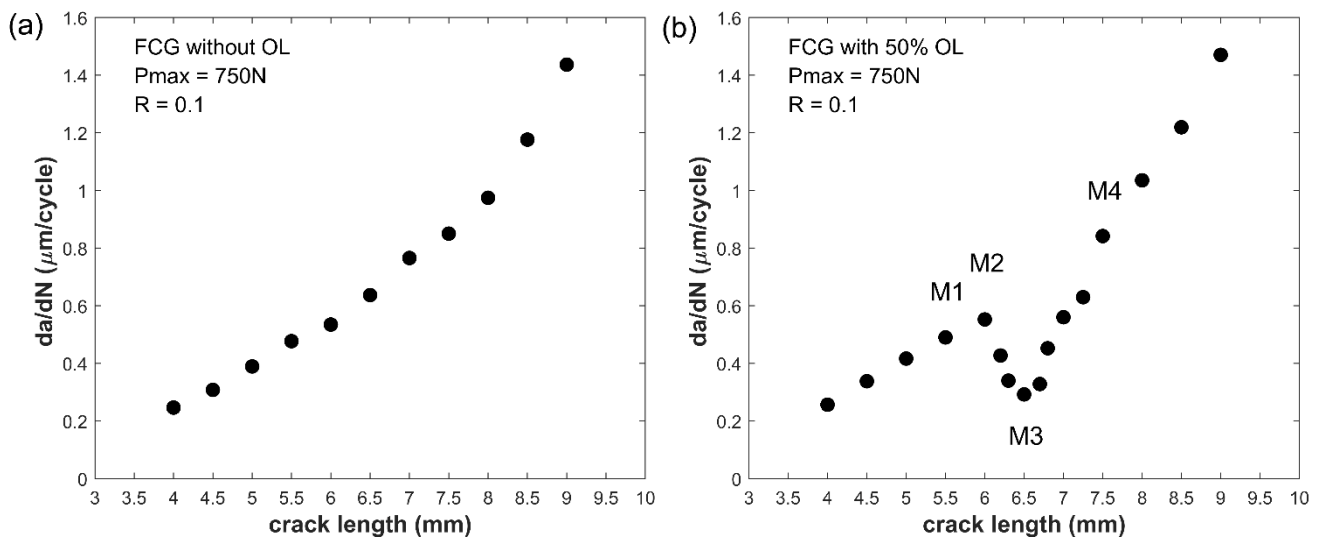


Figure 7. Crack growth rates vs crack length for samples without (a) and with (b) overload event.

Crack-tip opening displacement (CTOD) measurements at different crack lengths were taken to assess the effect of the overload application in the crack opening-closing mechanism. The analyzed points are shown in Figure 7b: points M1 and M2, before the OL application, represent crack lengths of 5.5 and 6 mm, respectively, the maximum retardation in growth rates occurs at point M3, which corresponds to a crack length of 6.5 mm, and lastly, the crack at point M4 has a length of 7.5 mm and is outside the OL-induced retardation zone. The results of this analysis are shown in Figure 8 corresponding to CTOD measurements obtained at 1 mm behind the crack tip. It can be seen that these curves exhibit similar behavior to the total CTOD curve presented in Figure 1 based on numerical predictions extracted from the first node at 8 μm behind the crack tip. Therefore, there is a portion of the CTOD curve corresponding to the unzipping of

crack flanks from the measurement point to the crack tip. This region is identified in Figure 8b from the minimum loading to a load of approximately 166 N, marked with a square. The slope that describes the elastic behavior of the material must be identified in the unloading portion of the curve, as indicated in Figure 8b. The translation of the curve to the loading part of the curve can be used to define the point marked with the square at which the crack is considered completely open. The same procedure was made in all CTOD measurements. It can be observed that the range of CTOD increases from M1 (see Figure 8a) to M2 (see Figure 8b) according to the increasing length of the crack. A small increase in elastic and plastic CTOD ranges is therefore expected. The crack opening levels are similar, i.e. $U^* = 17\%$ where U^* is the portion of the load cycle in which the crack surface is closed:

$$U^* = \frac{F_{open} - F_{min}}{F_{max} - F_{min}} \times 100 \quad (1)$$

where F_{open} is the crack opening load, and F_{min} and F_{max} are the minimum and maximum loads, respectively.

It can be observed that the crack opening level from the CTOD curve at the minimum FCG rate (point M3 in Figure 8c) is significantly higher $U^* = 43\%$, reducing the elastic and plastic CTOD ranges. According to the PICC model, as the crack propagated into the material following the overload, the greater response of the residual elastic ligaments over the plastic zones perturbed by the overload tends to compress it. This behavior reduces the crack opening-closing mechanism since a portion of the applied load is devoted to relieving the compressive loads transmitted through its faces as shown in CTOD curves of Figure 8c. Lastly, the CTOD curve at M4 (Figure 8d) exhibits similar behavior to the curves at M1 and M2, with low crack closure levels ($U^* = 19\%$). Relatively to M2, there is a significant increase in total CTOD, and consequently in plastic and elastic CTOD ranges. This increase in CTOD is explained by the effect of crack length on displacement fields. These experimental results indicated that the change in FCG rate produced by the imposition of the 50% overload is linked to the crack opening-closing mechanism. According to the literature, the effects of a single peak overload cycle are predominately due to residual stresses emerging in front of the crack tip [40], plasticity-induced crack closure acting on the crack surfaces behind the crack tip, or a combination of both. This phenomenon was recently studied by Borges et al. [12] through numerical simulations, verifying that the effect of overloads in FCG is mainly explained by plasticity-induced crack closure.

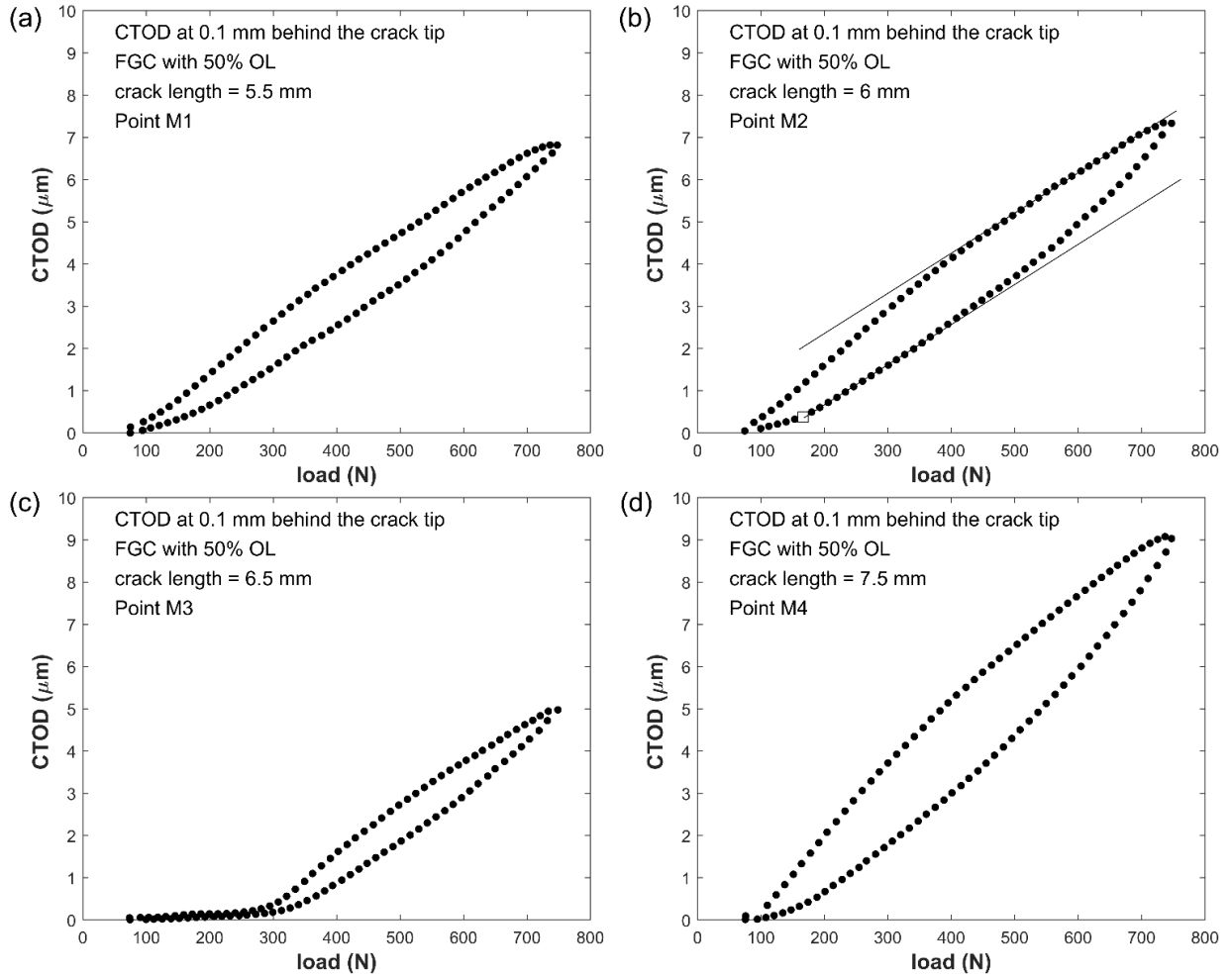


Figure 8. CTOD measurements by DIC analysis at different crack lengths for the sample with OL event: crack lengths of (a) 5.5 mm, (b) 6 mm, (c) 6.5 mm, and (d) 7.5 mm.

In the next analysis step, the methodology described in the previous section was applied to obtain the CTOD_p from the experimental data recorded from samples without and with overload events. Then, the plastic CTOD ranges were plotted versus the crack growth rates (da/dN) plotted in linear scales as shown in Figure 9. It can be seen that the relation ΔCTOD_p - da/dN obtained from the FCG with OL application follows a linear trend (see Figure 9b), similar to the non-OL case (see Figure 9a), taking into account the load sequence effects due to the imposed OL. As shown in Figure 9b, after the OL application at P1, the da/dN values begin to decrease following the linear trend depicted before the OL, and after reaching its minimum value at P2, da/dN values begin to increase following the same trend. The linear relationships for the crack growth rates of these fatigue tests are given by the following equations:

$$\frac{da}{dN} = 0.317 \times \Delta\text{CTOD}_p \quad (\text{without overload}) \quad (2)$$

$$\frac{da}{dN} = 0.338 \times \Delta CTOD_p \quad (\text{with overload}) \quad (3)$$

As expected, the constant α from equations 2 and 3 are very similar, showing that the equation $da/dN = \alpha \times \Delta CTOD_p$ takes into account the load sequence effects due to the imposed OL. Moreover, it is worth mentioning that both values of α are also in agreement with those obtained in previous work [32] conducted on the same material. Therefore, the constant α can be treated as an intrinsic property of the material. The small differences observed between them can be associated with the inherent scattering from experimental data and the methodology used to obtain the $CTOD_p$.

From these experimental results, despite the load sequence effects regarding the overload application, the $CTOD_p$ parameter has demonstrated a consistent correlation with crack growth rates. Moreover, its application is interesting because it allows for establishing a linear relationship with FCG rates in linear scales, independent of loading conditions.

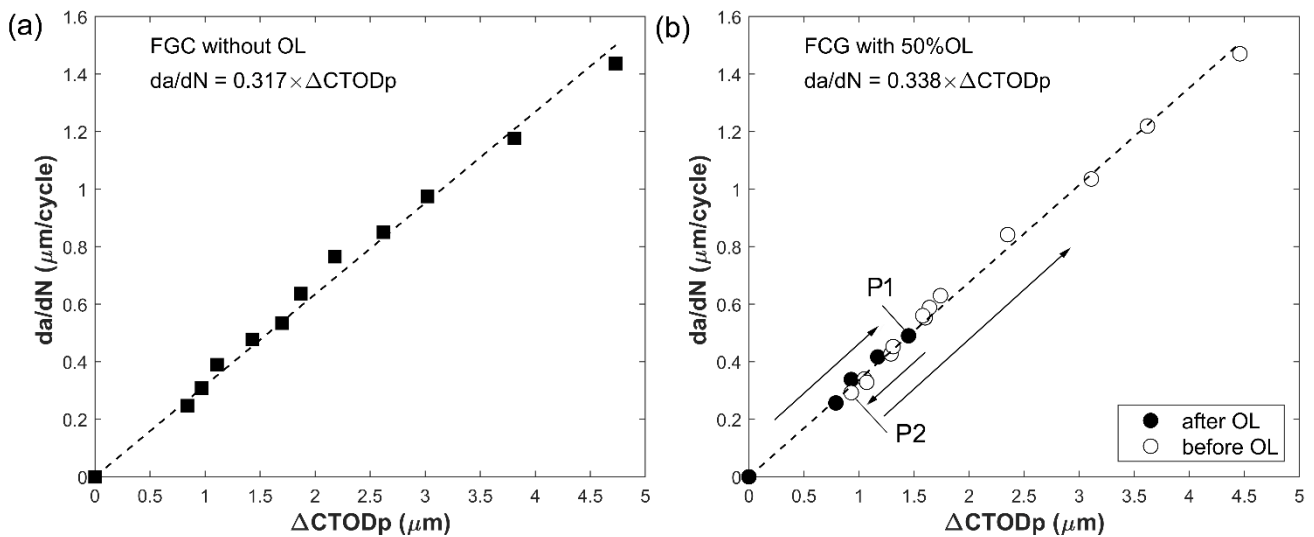


Figure 9. Plots of da/dN - $CTOD_p$ relationships for the two FCG tests (a) without and (b) with overload application.

Finally, the experimental data shown in Figure 10 is clear evidence of the good agreement between the $CTOD_p$ and the variations in FCG rates. It can be seen that the application of the 50% overload resulted in a transient effect that persisted for some extent until the crack grows beyond the region of influence caused by the overload. In fact, the minimum crack growth rate was registered after the crack grows for a period after the OL application, a phenomenon called delayed retardation that was correctly modeled by the $CTOD_p$. After reaching the maximum retardation, FCG rates begin to increase gradually and nonlinearly following typical retardation response for the plane stress case. The good correspondence between the FCG rates and $\Delta CTOD_p$ during the post-overload behavior is quite interesting because it

demonstrates that the $CTOD_p$ takes into account the mechanisms and related phenomena acting on the crack growth after the overload application.

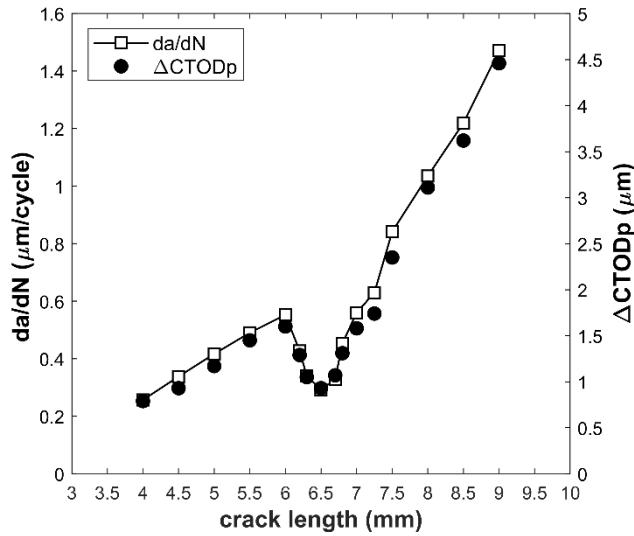


Figure 10. Plots of the da/dN and $\Delta CTOD_p$ versus crack length.

In order to visualize the effects of cycle interaction by the imposition of the single 50% OL, the variation of the crack-tip plastic zone during the post-overload propagation was characterized following the methods outlined in previous studies [41, 42]. From the experimental results presented in Figure 11a the following observations are made: (a) As expected, the OL induced an increase in the monotonic plastic zone size. (b) As the crack propagates inside the overload plastic zone, the interaction of the current plastic zone with the region perturbed by the overload can be observed, decreasing its size after OL application to maximum retardation reported at position OL+0.5 mm and increasing its size when getting away from this area. (c) It is clear that after reaching the maximum retardation, the size of the successive plastic zones increases as the crack leaves the region perturbed by the OL. (d) The extent of the overload plastic zone right of the crack tip is about 0.89 mm while positions OL+1 mm and OL+1.25 mm in the da/dN curve still indicate OL-induced effects acting in this region, as shown in Figure 11b. This could be expected because the crack closure phenomenon results from the residual plastic wake, so the crack tip must move some distance ahead of the region hypertrophied by the OL to disappear all its effects. It can be noted that all these cycle interaction effects were properly taken into account by the $CTOD_p$ following the linear relationship described by equation 3.

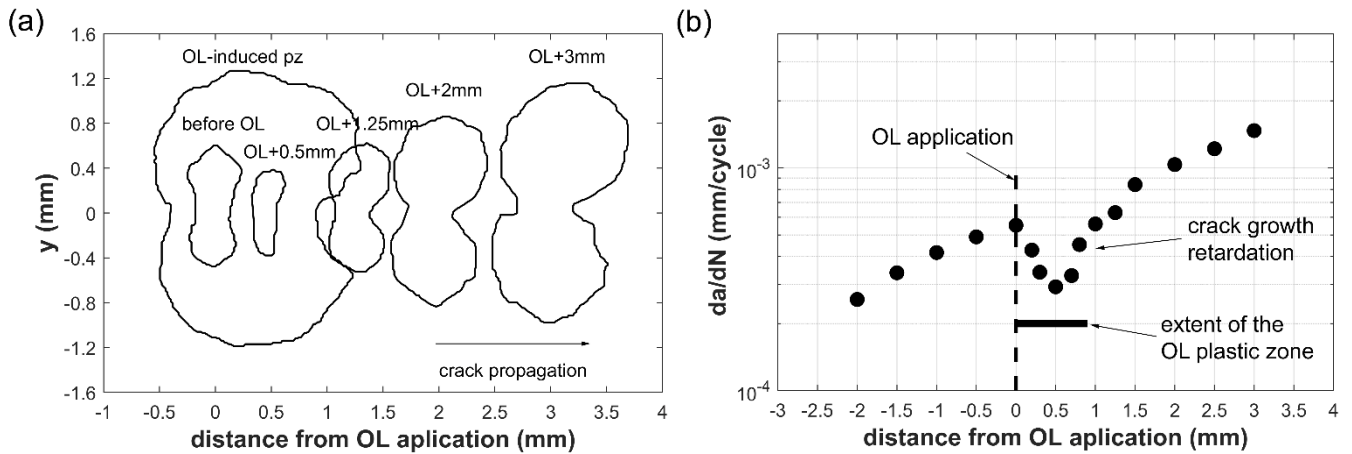


Figure 11. (a) Evolution of the plastic zone during the post-overload crack propagation. (b) FCG rates in logarithmic scale versus crack growth increment.

4. Discussion

The analysis of CTOD proved to be very useful because it can be used as a sensor of crack tip phenomena, namely, crack opening and closing, elastic deformation, and plastic deformation. The plastic deformation is quantified by subtracting the elastic component from the total CTOD, with its maximum value, $\Delta CTOD_p$, quantified at the maximum load. It is essential to emphasize that this parameter includes the effects of crack closure induced by plasticity, crack tip blunting, and residual stresses which are relevant in FCG under variable amplitude loading. In addition, the plastic CTOD has demonstrated a linear correlation with da/dN . This suggests that the primary damage mechanism responsible for FCG in Grade 2 titanium is crack-tip plastic deformation. The same conclusion was obtained in numerical and experimental studies. Neto et al. [43] found a good agreement between numerical predictions and experimental results obtained for MT specimens made of 6082-T6 aluminum alloy submitted to load blocks. Leitner et al. [44] examined nickel samples with grain sizes in the microcrystalline to the nanocrystalline range. In the near-threshold region up to the Paris regime, dislocation motion is the predominant damage mechanism, regardless of grain size, according to FCG measurements for various load ratios and extensive fracture surface analyses.

The linearity of da/dN versus $\Delta CTOD_p$ relation has been also observed in experimental results reported in previous studies for other materials, as shown in Figure 12. Therefore, the association between crack tip plastic deformation and FCG also occurs for other metallic materials. The variation of the α parameter of $da/dN = \alpha \times \Delta CTOD_p$ equation indicates that the same crack tip plastic deformation produces different crack extensions, depending on the material microstructure. Therefore, these results also suggest that the α parameter can be considered as an intrinsic material property.

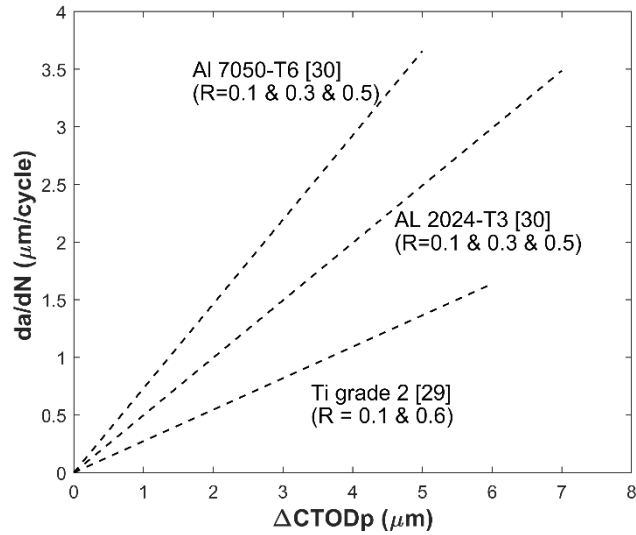


Figure 12. ΔCTOD_p vs da/dN curves for different materials from previous studies.

Finally, the mean stress effects in the ΔCTOD_p vs da/dN curves were also examined in this study by testing a sample with a different R-value. Figure 13 shows the results for an FCG conducted at $R = 0.3$. It can be observed that plotted data follows the same trend that the linear relationship previously defined for the material at $R = 0.1$. The fact that the crack closure is naturally included by the ΔCTOD_p parameter explains these experimental observations. Note that other phenomena, like partial closure, crack tip blunting, or damage below crack closure are also included in ΔCTOD_p . The ability to accommodate the effect of stress ratio has been widely used to validate crack driving parameters [45].

A recent paper [46] studied the variation of ΔK_{eff} and ΔCTOD_p along 3D curved crack fronts. The authors found equalized crack driving forces in terms of plastic CTOD along the crack front, which reinforces the ability of CTOD_p in the analysis of FCG.

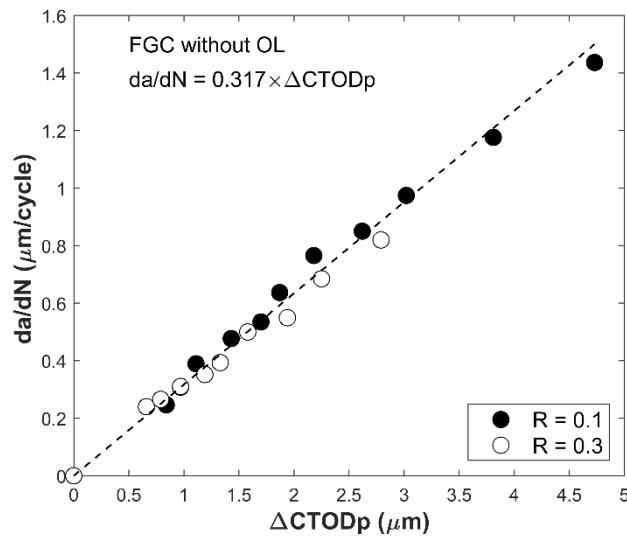


Figure 13. Plots of da/dN - ΔCTOD_p for tests conducted at different stress ratio values

5. Conclusions

An experimental study was conducted to examine the reliability of the viable use of plastic crack-tip opening displacement ($CTOD_p$) as a crack driving parameter for fatigue crack growth in a Grade 2 titanium sample following a single tensile overload. The main conclusions are:

- From the experimental results, the direct proportionality of the $\Delta CTOD_p$ vs da/dN curve was verified. It can be concluded that, for the test condition investigated, the OL-induced FCG retardation and related phenomena were naturally included in $\Delta CTOD_p$ measurements, prevailing the linear correspondence with fatigue crack growth rates.

It is worth emphasizing that $CTOD_p$ is a parameter, directly measured from the test, which establishes a link with the plastic deformation developed in front of the crack tip where the crack propagation occurs. Furthermore, it can be concluded that the primary damage mechanism responsible for FCG tests in Grade 2 titanium was the crack tip plastic deformation.

- The α parameter of $da/dN = \alpha \times \Delta CTOD_p$ relation changes with material, therefore it can be considered an intrinsic material property. In fact, the increase of the α parameter indicates that the same crack tip plastic deformation produces larger crack extensions, and this depends on the material microstructure.

- The $da/dN = \alpha \times \Delta CTOD_p$ relation is also independent of stress ratio in constant amplitude tests.

Therefore, these experimental results suggest the feasible use of the $CTOD_p$ as a driving force parameter for fatigue crack growth. In the future, it will be important to establish links between the α parameter and material microstructure. In fact, the α parameter quantifies the efficiency of crack tip plastic deformation in the production of crack growth, which is expected to be greatly dependent on microstructure. Additionally, it will be interesting to compare DIC measurements of plastic CTOD with numerical predictions obtained for plane stress and plane strain states, which is important for a better understanding of the effect of thickness on surface measurements.

Acknowledgments

The authors would like to acknowledge the financial support from Ministerio de Universidades del Gobierno de España through the program “Recualificación del Sistema Universitario Español 2021-2023: ayudas Maria Zambrano”, the Junta de Andalucía through the research project “1380786” funded by the program “Proyectos de I + D + i en el Marco del Programa Operativo FEDER Andalucía 2014-2020, also the portuguese funds through FCT-Fundação para a Ciência e a Tecnologia –, under the project UIDB/00285/2020.

References

- [1] J.R. Rice, The mechanics of crack tip deformation and extension by fatigue, Division of Engineering, Brown University, 1966, <https://doi.org/10.1520/stp47234s>
- [2] W. Elber, The significance of fatigue crack closure, (1971), <https://doi.org/10.1520/stp26680s>
- [3] E. Von Euw, R. Hertzberg, R. Roberts, Delay effects in fatigue crack propagation, *Astm Stp*, 513 (1972) 230-259, <https://doi.org/10.1520/STP34123S>
- [4] C. Shin, N. Fleck, Overload retardation in a structural steel, *Fatigue & Fracture of Engineering Materials & Structures*, 9 (1987) 379-393, <https://doi.org/10.1111/j.1460-2695.1987.tb00464.x>
- [5] W. Mills, R. Hertzberg, The effect of sheet thickness on fatigue crack retardation in 2024-T3 aluminum alloy, *Engineering Fracture Mechanics*, 7 (1975) 705-711, [https://doi.org/10.1016/0013-7944\(75\)90026-0](https://doi.org/10.1016/0013-7944(75)90026-0)
- [6] C. Shin, S. Hsu, On the mechanisms and behaviour of overload retardation in AISI 304 stainless steel, *International Journal of Fatigue*, 15 (1993) 181-192, [https://doi.org/10.1016/0142-1123\(93\)90175-p](https://doi.org/10.1016/0142-1123(93)90175-p)
- [7] K. Sadananda, A. Vasudevan, R. Holtz, E. Lee, Analysis of overload effects and related phenomena, *International Journal of Fatigue*, 21 (1999) S233-S246, [https://doi.org/10.1016/s0142-1123\(99\)00094-8](https://doi.org/10.1016/s0142-1123(99)00094-8)
- [8] R. Pippan, A. Hohenwarter, Fatigue crack closure: a review of the physical phenomena, *Fatigue & fracture of engineering materials & structures*, 40 (2017) 471-495, <https://doi.org/10.1111/ffe.12578>
- [9] P. Paris, F. Erdogan, A critical analysis of crack propagation laws, (1963), <https://doi.org/10.1115/1.3656900>
- [10] D. Kujawski, Discussion and Comments on KOP and ΔK_{eff} , *Materials*, 2020, pp. 4959, <https://doi.org/10.3390/ma13214959>
- [11] M.F. Borges, D.M. Neto, F.V. Antunes, Revisiting classical issues of fatigue crack growth using a non-linear approach, *Materials*, 13 (2020) 5544, <https://doi.org/10.3390/ma13235544>
- [12] J.A.O. González, J.T.P. de Castro, M.A. Meggiolaro, G.L.G. Gonzáles, J.L. de Franca Freire, Challenging the “ ΔK_{eff} is the driving force for fatigue crack growth” hypothesis, *International Journal of Fatigue*, 136 (2020) 105577, <https://doi.org/10.1016/j.ijfatigue.2020.105577>
- [13] D. Kujawski, On assumptions associated with ΔK_{eff} and their implications on FCG predictions, *International journal of fatigue*, 27 (2005) 1267-1276, <https://doi.org/10.1016/j.ijfatigue.2005.07.020>
- [14] K. Sadananda, D.-N.V. Ramaswamy, Role of crack tip plasticity in fatigue crack growth, *Philosophical Magazine A*, 81 (2001) 1283-1303, <https://doi.org/10.1080/01418610108214441>
- [15] F. Antunes, T. Sousa, R. Branco, L. Correia, Effect of crack closure on non-linear crack tip parameters, *International Journal of Fatigue*, 71 (2015) 53-63, <https://doi.org/10.1016/j.ijfatigue.2014.10.001>
- [16] J. Pokluda, Dislocation-based model of plasticity and roughness-induced crack closure, *International journal of fatigue*, 46 (2013) 35-40, <https://doi.org/10.1016/j.ijfatigue.2011.11.016>

- [17] H. Chen, W. Chen, T. Li, J. Ure, Effect of circular holes on the ratchet limit and crack tip plastic strain range in a centre cracked plate, *Engineering fracture mechanics*, 78 (2011) 2310-2324, <https://doi.org/10.1016/j.engfracmech.2011.05.004>
- [18] H.-B. Park, K.-M. Kim, B.-W. Lee, Plastic zone size in fatigue cracking, *International journal of pressure vessels and piping*, 68 (1996) 279-285, [https://doi.org/10.1016/0308-0161\(95\)00066-6](https://doi.org/10.1016/0308-0161(95)00066-6)
- [19] J.-Z. Zhang, J.-Z. Zhang, S.Y. Du, Elastic-plastic finite element analysis and experimental study of short and long fatigue crack growth, *Engineering Fracture Mechanics*, 68 (2001) 1591-1605, [https://doi.org/10.1016/s0013-7944\(01\)00047-9](https://doi.org/10.1016/s0013-7944(01)00047-9)
- [20] S. Bodner, D. Davidson, J. Lankford, A description of fatigue crack growth in terms of plastic work, *Engineering Fracture Mechanics*, 17 (1983) 189-191, [https://doi.org/10.1016/0013-7944\(83\)90169-8](https://doi.org/10.1016/0013-7944(83)90169-8)
- [21] N.W. Klingbeil, A total dissipated energy theory of fatigue crack growth in ductile solids, *International Journal of Fatigue*, 25 (2003) 117-128, [https://doi.org/10.1016/s0142-1123\(02\)00073-7](https://doi.org/10.1016/s0142-1123(02)00073-7)
- [22] L. Campbell. The influence of metallurgical structure on the mechanisms of fatigue crack propagation. *ASTM STP 415 (1967): 131-168*, <https://doi.org/10.1520/STP47230S>
- [23] R. N. Pelloux. Crack extension by alternating shear. *Engineering Fracture Mechanics*, 1 (1970), 697-704, [https://doi.org/10.1016/0013-7944\(70\)90008-1](https://doi.org/10.1016/0013-7944(70)90008-1)
- [24] P. Neumann. The geometry of slip processes at a propagating fatigue crack—II. *Acta Metallurgica* 22.9 (1974): 1167-1178, [https://doi.org/10.1016/0001-6160\(74\)90072-8](https://doi.org/10.1016/0001-6160(74)90072-8)
- [25] V. Tvergaard, On fatigue crack growth in ductile materials by crack-tip blunting, *Journal of the Mechanics and Physics of Solids*, 52 (2004) 2149-2166, <https://doi.org/10.1016/j.jmps.2004.02.007>
- [26] R. Pippan, W. Grosinger, Fatigue crack closure: From LCF to small scale yielding, *International journal of fatigue*, 46 (2013) 41-48, <https://doi.org/10.1016/j.ijfatigue.2012.02.016>
- [27] W. Guo, C. Wang, L. Rose, The influence of cross-sectional thickness on fatigue crack growth, *Fatigue & Fracture of Engineering Materials & Structures*, 22 (1999) 437-444, <https://doi.org/10.1046/j.1460-2695.1999.00176.x>
- [28] A. Ktari, M. Baccar, M. Shah, N. Haddar, H. Ayedi, F. Rezai-Aria, A crack propagation criterion based on Δ CTOD measured with 2D-digital image correlation technique, *Fatigue & Fracture of Engineering Materials & Structures*, 37 (2014) 682-694, <https://doi.org/10.1111/ffe.12153>
- [29] A. Shahani, H.M. Kashani, M. Rastegar, M.B. Dehkordi, A unified model for the fatigue crack growth rate in variable stress ratio, *Fatigue & Fracture of Engineering Materials & Structures*, 32 (2009) 105-118, <https://doi.org/10.1111/j.1460-2695.2008.01315.x>
- [30] F. Antunes, S. Rodrigues, R. Branco, D. Camas, A numerical analysis of CTOD in constant amplitude fatigue crack growth, *Theoretical and Applied Fracture Mechanics*, 85 (2016) 45-55, <https://doi.org/10.1016/j.tafmec.2016.08.015>

- [31] F. Antunes, R. Branco, P. Prates, L. Borrego, Fatigue crack growth modelling based on CTOD for the 7050-T6 alloy, *Fatigue & Fracture of Engineering Materials & Structures*, 40 (2017) 1309-1320, <https://doi.org/10.1111/ffe.12582>
- [32] J. Vasco-Olmo, F. Díaz, F. Antunes, M. James, Characterisation of fatigue crack growth using digital image correlation measurements of plastic CTOD, *Theoretical and Applied Fracture Mechanics*, 101 (2019) 332-341, <https://doi.org/10.1016/j.tafmec.2019.03.009>
- [33] J.M. Vasco-Olmo, F.A. Diaz Garrido, F.V. Antunes, M. James, Plastic CTOD as fatigue crack growth characterising parameter in 2024-T3 and 7050-T6 aluminium alloys using DIC, *Fatigue & Fracture of Engineering Materials & Structures*, 43 (2020) 1719-1730, <https://doi.org/10.1111/ffe.13210>
- [34] G.L. Gonzales, J.A. Gonzalez, J.L. Freire, Characterization of discontinuous crack closure behavior after the application of a single overload cycle, *Theoretical and Applied Fracture Mechanics*, 114 (2021) 103028, <https://doi.org/10.1016/j.tafmec.2021.103028>
- [35] D. Nowell, P. De Matos, Application of digital image correlation to the investigation of crack closure following overloads, *Procedia Engineering*, 2 (2010) 1035-1043, <https://doi.org/10.1016/j.proeng.2010.03.112>
- [36] Gonzáles, G. L. G., González, J. A. O., Castro, J. T. P., & Freire, J. L. F. Detecting fatigue crack closure and crack growth delays after an overload using DIC measurements. In *Fracture, Fatigue, Failure and Damage Evolution, Volume 7: Proceedings of the 2017 Annual Conference on Experimental and Applied Mechanics*, Springer International Publishing. (2018) pp. 57-65, https://doi.org/10.1007/978-3-319-62831-8_8
- [37] Gonzáles, G. L. G., González, J. A. O., Neto, D. M., Antunes, F. V., & Díaz, F. A. Experimental determination of the reversed plastic zone size around fatigue crack using Digital Image Correlation. *Theoretical and Applied Fracture Mechanics*, (2023) 103901, <https://doi.org/10.1016/j.tafmec.2023.103901>
- [38] International Digital Image Correlation Society, Jones, E.M.C. and Iadicola, M.A. (Eds.) (2018). *A Good Practices Guide for Digital Image Correlation*, <https://doi.org/10.32720/idics/gpg.ed1/print.format>
- [39] G. Gonzáles, J. Diaz, J. González, J. Castro, J.d.F. Freire, Determining SIFs using DIC considering crack closure and blunting, in: *Experimental and Applied Mechanics, Volume 4*, Springer, 2017, pp. 25-36, https://doi.org/10.1007/978-3-319-42028-8_4
- [40] E. Salvati, S. O'connor, T. Sui, D. Nowell, A. Korsunsky, A study of overload effect on fatigue crack propagation using EBSD, FIB–DIC and FEM methods, *Engineering Fracture Mechanics*, 167 (2016) 210-223, <https://doi.org/10.1016/j.engfracmech.2016.04.034>
- [41] J. Vasco-Olmo, M. James, C. Christopher, E. Patterson, F. Díaz, Assessment of crack tip plastic zone size and shape and its influence on crack tip shielding, *Fatigue & Fracture of Engineering Materials & Structures*, 39 (2016) 969-981, <https://doi.org/10.1111/ffe.12436>
- [42] G. Gonzáles, J. González, V. Paiva, J. Freire, Crack-tip plastic zone size and shape via DIC, in: *Fracture, Fatigue, Failure and Damage Evolution, Volume 6*, Springer, 2019, pp. 5-10, https://doi.org/10.1007/978-3-319-95879-8_2

- [43] D. Neto, E. Sérgio, M. Borges, L. Borrego, F. Antunes, Effect of load blocks on fatigue crack growth, *International Journal of Fatigue*, 162 (2022) 107001, <https://doi.org/10.1016/j.ijfatigue.2022.107001>
- [44] T. Leitner, A. Hohenwarter, R. Pippan, Revisiting fatigue crack growth in various grain size regimes of Ni, *Materials Science and Engineering: A*, 646 (2015) 294-305, <https://doi.org/10.1016/j.msea.2015.08.071>
- [45] Daniel Kujawski, A fatigue crack driving force parameter with load ratio effects, *International Journal of Fatigue* 23 (2001) S239–S246, [https://doi.org/10.1016/S0142-1123\(01\)00158-X](https://doi.org/10.1016/S0142-1123(01)00158-X)
- [46] T. Oplt, T. Vojtek, R. Kubíček, P. Pokorný, P. Hutař, Numerical modelling of fatigue crack closure and its implication on crack front curvature using $\Delta CTOD_p$, *International Journal of Fatigue*, (2023) 107570, <https://doi.org/10.1016/j.ijfatigue.2023.107570>

G.L. Gómez Gonzales: Methodology, Investigation, Writing - Original Draft, Writing - Review & Editing. Jose M. Vasco-Olmo: Conceptualization, Methodology, Investigation. F.V. Antunes: Methodology, Writing - Review & Editing. D.M. Neto: Methodology, Visualization. F.A. Diaz: Methodology, Supervision. All the authors contributed to its final version through their critical comments, editions, and reviews.